

EFFICIENT AND ACCURATE EXPLANATION ESTIMATION WITH DISTRIBUTION COMPRESSION

Hubert Baniecki

University of Warsaw
h.baniecki@uw.edu.pl

Giuseppe Casalicchio

LMU Munich
Munich Center for Machine Learning

Bernd Bischl

LMU Munich
Munich Center for Machine Learning

Przemyslaw Biecek

University of Warsaw
Warsaw University of Technology

ABSTRACT

We discover a theoretical connection between explanation estimation and distribution compression that significantly improves the approximation of feature attributions, importance, and effects. While the exact computation of various machine learning explanations requires numerous model inferences and becomes impractical, the computational cost of approximation increases with an ever-increasing size of data and model parameters. We show that the standard i.i.d. sampling used in a broad spectrum of algorithms for post-hoc explanation leads to an approximation error worthy of improvement. To this end, we introduce *compress then explain* (CTE), a new paradigm of sample-efficient explainability. It relies on distribution compression through kernel thinning to obtain a data sample that best approximates its marginal distribution. CTE significantly improves the accuracy and stability of explanation estimation with negligible computational overhead. It often achieves an on-par explanation approximation error 2–3× faster by using fewer samples, i.e. requiring 2–3× fewer model evaluations. CTE is a simple, yet powerful, plug-in for any explanation method that now relies on i.i.d. sampling.

1 INTRODUCTION

Computationally efficient estimation of post-hoc explanations is at the forefront of current research on explainable machine learning (Strumbelj & Kononenko, 2010; Slack et al., 2021; Jethani et al., 2022; Chen et al., 2023; Donnelly et al., 2023; Muschalik et al., 2024). The majority of the work focuses on improving efficiency with respect to the dimension of features (Covert et al., 2020; Jethani et al., 2022; Chen et al., 2023; Fumagalli et al., 2023), specific model classes like neural networks (Erion et al., 2021; Chen et al., 2024) and decision trees (Muschalik et al., 2024), or approximating the conditional feature distribution (Chen et al., 2018; Aas et al., 2021; Olsen et al., 2022; 2024).

However, in many practical settings, a marginal feature distribution is used instead to estimate explanations, and i.i.d. samples from the data typically form the so-called *background data* samples, also known as *reference points* or *baselines*, which plays a crucial role in the estimation process (Lundberg & Lee, 2017; Scholbeck et al., 2020; Erion et al., 2021; Ghalebikesabi et al., 2021; Lundstrom et al., 2022). For example, Covert et al. (2020) mention “[O]ur sampling approximation for SAGE was run using draws from the marginal distribution. We used a fixed set of 512 background samples [...]” and we provide more such references in Appendix A to motivate our research question: *Can we reliably improve on standard i.i.d. sampling in explanation estimation?*

We make a connection to research on statistical theory, where kernel thinning (KT, Dwivedi & Mackey, 2021; 2022) was introduced to compress a distribution more effectively than with i.i.d. sampling. KT has an efficient implementation in the COMPRESS++ algorithm (Shetty et al., 2022) and was applied to improve statistical kernel testing (Domingo-Enrich et al., 2023). Building on this line of work, this paper aims to thoroughly quantify the error introduced by the current *sample then explain* paradigm in feature marginalization, which is involved in the estimation of both local and global removal-based explanations (Covert et al., 2021). We propose an efficient way to reduce this approximation error based on distribution compression (Figure 1).

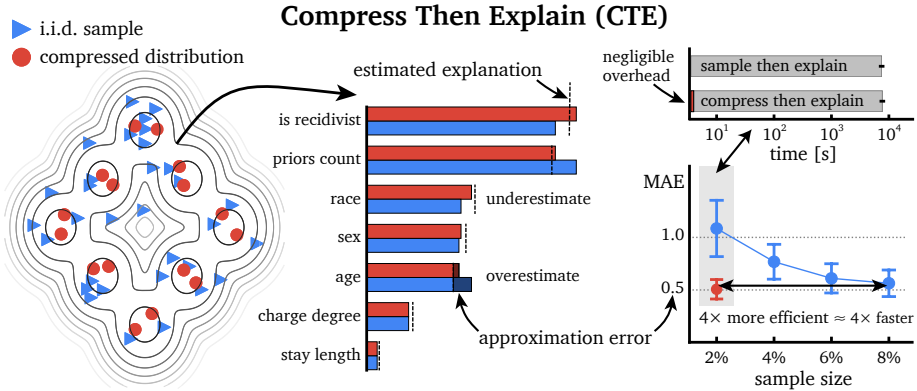


Figure 1: Garbage sample in, garbage explanation out. *Sample then explain* is a conventional approach to decrease the computational cost of explanation estimation. Although fast, sampling is inefficient and prone to error, which may even lead to changes in feature importance rankings. We propose *compress then explain* (CTE), a new paradigm for accurate, yet efficient, estimation of explanations based on a marginal distribution that is compressed, e.g. with kernel thinning.

Contribution. In summary, our work advances literature in multiple ways: **(1) Quantifying the error of standard i.i.d. sampling:** We bring to attention and measure the approximation error introduced by using i.i.d. sampling of background and foreground data in various explanation methods. It may even lead to changes in feature importance rankings. **(2) Compress then explain (CTE):** We introduce a new paradigm of sample-efficient explainability where post-hoc explanations, like feature attributions and effects, are estimated based on a marginal distribution compressed more efficiently than with i.i.d. sampling. CTE is theoretically justified as we discover a connection between explanation estimation and distribution compression. **(3) Kernel thinning for (explainable) machine learning:** We show empirically that KT outperforms i.i.d. sampling in compressing the distribution of popular datasets used in research on explainable machine learning. In fact, this is the first work to evaluate distribution compression via KT on datasets for supervised learning, which itself is valuable. **(4) Decreasing the computational cost of explanation estimation:** We benchmark *compress then explain* (CTE) with popular explanation methods and show it results in more accurate explanations of smaller variance. CTE often achieves on-par error using 2–3 \times fewer samples, i.e. requiring 2–3 \times fewer model inferences. CTE is a simple, yet powerful, plug-in for a broad class of methods that sample from a dataset, e.g. removal-based and global explanations.

Related work. Our work is the first to empirically evaluate KT on datasets for supervised learning, and one of the first to reliably improve on i.i.d. sampling for multiple post-hoc explanation methods at once. Laberge et al. (2023) propose a biased sampling algorithm to attack the estimation of feature attributions, which further motivates finding robust improvements for i.i.d. sampling. Our research question is orthogonal to that of *how to sample perturbations around an input* (Petsiuk et al., 2018; Slack et al., 2021; Li et al., 2021; Ghalebikesabi et al., 2021; Li et al., 2023), or *how to efficiently sample feature coalitions* (Chen et al., 2018; Covert & Lee, 2021; Fumagalli et al., 2023). Instead of generating samples from the conditional distribution itself, which is challenging (Olsen et al., 2022), we explore how to efficiently select an appropriate subset of background data for explanations (Hase et al., 2021; Lundstrom et al., 2022). Specifically for Shapley-based explanations, Jethani et al. (2022) propose to predict them with a learned surrogate model, while Kolpaczki et al. (2024) propose their representation detached from the notion of marginal contribution. We aim to propose a general paradigm shift that benefits a broader class of explanation methods including feature effects (Apley & Zhu, 2020; Moosbauer et al., 2021) and expected gradients (Erion et al., 2021; Zhang et al., 2024).

Concerning distribution compression, the method most related to KT (Dwivedi & Mackey, 2021) is the inferior standard thinning approach (Owen, 2017). Cooper et al. (2023) use insights from KT to accelerate distributed training, while Zimmerman et al. (2024) apply KT in robotics. In the context of data-centric machine learning, we broadly relate to finding coresets to improve the efficiency of clustering (Agarwal et al., 2004; Har-Peled & Mazumdar, 2004) and active learning (Sener & Savarese, 2018), as well as dataset distillation (Wang et al., 2018) and dataset condensation (Zhao et al., 2021; Kim et al., 2022) that create synthetic samples to improve the efficiency of model training.

2 PRELIMINARIES

We aim to explain a prediction model trained on labeled data and denoted by $f: \mathcal{X} \mapsto \mathbb{R}$ where \mathcal{X} is the feature space; it predicts an output using an input feature vector \mathbf{x} . Usually, we assume $\mathcal{X} \subseteq \mathbb{R}^d$. Without loss of generality, in the case of classification, we explain the output of a single class as a posterior probability from $[0, 1]$. We can assume a given dataset $\{(\mathbf{x}^{(1)}, y^{(1)}), \dots, (\mathbf{x}^{(n)}, y^{(n)})\}$, where every element comes from $\mathcal{X} \times \mathcal{Y}$, the underlying feature and label space, on which the explanations are computed. Depending on the explanation method and scenario, the dataset could be provided without labels. We denote such $n \times d$ dimensional dataset by \mathbb{X} where $\mathbf{x}^{(i)}$ appears in the i -th row of \mathbb{X} , which is assumed to be sampled in an i.i.d. fashion from an underlying distribution $p(\mathbf{x}, y)$ defined on $\mathcal{X} \times \mathcal{Y}$. We denote a random vector as $\mathbf{X} \in \mathcal{X}$. Further, let $s \subset \{1, \dots, d\}$ be a feature index set of interest with its complement $\bar{s} = \{1, \dots, d\} \setminus s$. We index feature vectors \mathbf{x} and random variables \mathbf{X} by index set s to restrict them to these index sets. We write $p_{\mathbf{X}}(\mathbf{x})$ and $p_{\mathbf{X}_s}(\mathbf{x}_s)$ for marginal distributions on \mathbf{X} and \mathbf{X}_s , respectively, and $p_{\mathbf{X}_s|\mathbf{X}_t}(\mathbf{x}_s|\mathbf{x}_t)$ for conditional distribution on $\mathbf{X}_s|\mathbf{X}_t$. We use $q_{\mathbb{X}}$ to denote an empirical distribution approximating $p_{\mathbf{X}}$ based on a dataset \mathbb{X} .

2.1 SAMPLING FROM THE DATASET IS PREVALENT IN EXPLANATION ESTIMATION

Various estimators of post-hoc explanations sample from the dataset to efficiently approximate the explanation estimate (Appendix A). For example, many removal-based explanations (Covert et al., 2021) like SHAP (Lundberg & Lee, 2017) and SAGE (Covert et al., 2020) rely on marginalizing features out of the model function f using their joint conditional distribution $\mathbb{E}_{\mathbf{X}_{\bar{s}} \sim p_{\mathbf{X}_{\bar{s}}|\mathbf{X}_s=\mathbf{x}_s}}[f(\mathbf{x}_s, \mathbf{X}_{\bar{s}})] = \int f(\mathbf{x}_s, \mathbf{x}_{\bar{s}}) p_{\mathbf{X}_{\bar{s}}|\mathbf{X}_s=\mathbf{x}_s}(\mathbf{x}_{\bar{s}}|\mathbf{x}_s) d\mathbf{x}_{\bar{s}}$. Note that the practical approximation of the conditional distribution $p_{\mathbf{X}_{\bar{s}}|\mathbf{X}_s=\mathbf{x}_s}(\mathbf{x}_{\bar{s}}|\mathbf{x}_s)$ itself is challenging (Chen et al., 2018; Aas et al., 2021; Olsen et al., 2022) and there is no ideal solution to this problem (see a recent benchmark by Olsen et al., 2024). For example, the default for SAGE is to assume feature independence and use the marginal distribution $p_{\mathbf{X}_{\bar{s}}|\mathbf{X}_s=\mathbf{x}_s}(\mathbf{x}_{\bar{s}}|\mathbf{x}_s) := p_{\mathbf{X}_{\bar{s}}}(\mathbf{x}_{\bar{s}})$ (Covert et al., 2020, Appendix D); so does the KERNEL-SHAP estimator, i.e. a practical implementation of SHAP (Lundberg & Lee, 2017). This trend continues in more recent work sampling from marginal distribution (Fumagalli et al., 2023; Krzyżiński et al., 2023).

Definition 1 (Feature marginalization). *Given a set of observed values \mathbf{x}_s , we define a model function with marginalized features from the set \bar{s} as $f(\mathbf{x}_s; \mathbf{p}_{\mathbf{X}_{\bar{s}}}) := \mathbb{E}_{\mathbf{X}_{\bar{s}} \sim p_{\mathbf{X}_{\bar{s}}}}[f(\mathbf{x}_s, \mathbf{X}_{\bar{s}})]$.*

In practice, the expectation $\mathbb{E}_{\mathbf{X}_{\bar{s}} \sim p_{\mathbf{X}_{\bar{s}}}}[f(\mathbf{x}_s, \mathbf{X}_{\bar{s}})]$ is estimated by i.i.d. sampling from the dataset \mathbb{X} that approximates the distribution $p_{\mathbf{X}_{\bar{s}}}(\mathbf{x}_{\bar{s}})$. This sampled set of points forms the so-called *background data*, aka *reference points*, or *baselines* as specifically in case of the expected gradients (Erion et al., 2021) explanation method, which can be defined as $\text{EXPECTED-GRADIENTS}(\mathbf{x}) := \mathbb{E}_{\mathbf{X} \sim p_{\mathbf{X}}, \alpha \sim U(0,1)} \left[(\mathbf{x} - \mathbf{X}) \cdot \frac{\partial f(\mathbf{X} + \alpha \cdot (\mathbf{x} - \mathbf{X}))}{\partial \mathbf{X}} \right]$. Klein et al. (2024) benchmark feature attribution methods showing that EXPECTED-GRADIENTS is among the most faithful and robust ones.

Furthermore, i.i.d. sampling is used in global explanation methods, many of which are an *aggregation* of local explanations. To improve the computational efficiency of these approximations, often only a subset of \mathbb{X} is considered, called *foreground data*. Examples include: FEATURE-EFFECTS explanations (Apley & Zhu, 2020), an aggregation of LIME (Ribeiro et al., 2016) into G-LIME (Li et al., 2023), and again SAGE, for which points from \mathbb{X} require to have their corresponding labels y .

2.2 BACKGROUND ON DISTRIBUTION COMPRESSION

Standard sampling strategies can be inefficient (Dwivedi & Mackey, 2021). For example, the Monte Carlo estimate $\frac{1}{n} \sum_{i=1}^n h(\mathbf{x}^{(i)})$ of an unknown expectation $\mathbb{E}_{\mathbf{X} \sim p_{\mathbf{X}}} h(\mathbf{X})$ based on n i.i.d. points has $\Theta(1/\sqrt{n})$ integration error $|\mathbb{E}_{\mathbf{X} \sim p_{\mathbf{X}}} h(\mathbf{X}) - \frac{1}{n} \sum_{i=1}^n h(\mathbf{x}^{(i)})|$ requiring 10^2 points for 10% relative error and 10^4 points for 1% error (Shetty et al., 2022). To improve on i.i.d. sampling, given a sequence \mathbb{X} of n input points summarizing a target distribution $p_{\mathbf{X}}$, the goal of distribution compression is to identify a high quality *coreset* $\tilde{\mathbb{X}}$ of size $\tilde{n} \ll n$. This quality is measured with the coreset’s integration error $|\frac{1}{n} \sum_{i=1}^n h(\mathbf{x}^{(i)}) - \frac{1}{\tilde{n}} \sum_{i=1}^{\tilde{n}} h(\tilde{\mathbf{x}}^{(i)})|$ for functions h in the reproducing kernel Hilbert space induced by a given kernel function \mathbf{k} (Muandet et al., 2017). The recently introduced KT algorithm (Dwivedi & Mackey, 2021; 2022) returns such a coreset that minimizes the kernel maximum mean discrepancy (MMD _{\mathbf{k}} , Gretton et al., 2012).

Definition 2 (Kernel maximum mean discrepancy (Gretton et al., 2012; Dwivedi & Mackey, 2021)). Let $\mathbf{k} : \mathbb{R}^d \times \mathbb{R}^d \mapsto \mathbb{R}$ be a bounded kernel function with $\mathbf{k}(\mathbf{x}, \cdot)$ measurable for all $\mathbf{x} \in \mathbb{R}^d$, e.g. a Gaussian kernel. Kernel maximum mean discrepancy between probability distributions p, q on \mathbb{R}^d is defined as $\text{MMD}_{\mathbf{k}}(p, q) := \sup_{h \in \mathcal{H}_{\mathbf{k}} : \|h\|_{\mathbf{k}} \leq 1} |\mathbb{E}_{\mathbf{X} \sim p_{\mathbf{X}}} h(\mathbf{X}) - \mathbb{E}_{\mathbf{X} \sim q_{\mathbf{X}}} h(\mathbf{X})|$, where $\mathcal{H}_{\mathbf{k}}$ is a reproducing kernel Hilbert induced by \mathbf{k} .

To formulate Propositions 1 & 2 in the next Section, we recall a biased estimate of maximum mean discrepancy, which is discussed in (Chérif-Abdellatif & Alquier, 2022, remark 3.2) and (Sriperumbudur et al., 2010, corollary 4).

Definition 3 (Biased estimator of $\text{MMD}_{\mathbf{k}}$). From (Muandet et al., 2017, section 5.1), as shown in (Gretton et al., 2012), the L_2 distance between kernel density estimates $p_{\mathbb{X}}, q_{\mathbb{X}}$ is a special case of the biased $\text{MMD}_{\mathbf{k}}$ estimator, i.e. we have $\widehat{\text{MMD}}_{\mathbf{k}}^2(p_{\mathbb{X}}, q_{\mathbb{X}}) := \|p_{\mathbb{X}} - q_{\mathbb{X}}\|_2^2 = \int (p_{\mathbf{X}}(\mathbf{x}) - q_{\mathbf{X}}(\mathbf{x}))^2 d\mathbf{x}$.

An unbiased empirical estimate of $\text{MMD}_{\mathbf{k}}$ can be relatively easily computed given a kernel function \mathbf{k} (Gretton et al., 2012). COMPRESS++ (Shetty et al., 2022) is an efficient algorithm for KT that returns a coreset of size \sqrt{n} in $\mathcal{O}(n \log^3 n)$ time and $\mathcal{O}(\sqrt{n} \log^2 n)$ space, making KT viable for large datasets. It was adapted to improve the kernel two-sample test (Domingo-Enrich et al., 2023).

3 COMPRESS THEN EXPLAIN (CTE)

We propose distribution compression as a substitute to i.i.d. sampling for feature marginalization in removal-based explanations and for aggregating global explanations. We now formalize the problem and provide theoretical intuition as to why methods for distribution compression can lead to more accurate explanation estimates. We defer the proofs to Appendix B.

Definition 4 (Local explanation based on feature marginalization). A local explanation is a function $g(\mathbf{x}; f, p_{\mathbf{X}}) : \mathcal{X} \mapsto \mathbb{R}^p$ of input \mathbf{x} given model f that relies on a distribution $p_{\mathbf{X}}$ for feature marginalization. For estimation, it uses an empirical distribution $q_{\mathbb{X}}$ in place of $p_{\mathbf{X}}$.

Examples of such local explanations include SHAP (Lundberg & Lee, 2017) and EXPECTED-GRADIENTS (Erion et al., 2021). We aim to provide high-quality explanations stemming from compressed samples as measured with a given approximation error, e.g. mean absolute error.

Problem formulation. To optimize the approximation error, we propose a novel formulation of the sample selection problem:

$$\begin{aligned} \min_{\tilde{\mathbb{X}}} \quad & \|g(\mathbf{x}; f, q_{\tilde{\mathbb{X}}}) - g(\mathbf{x}; f, q_{\mathbb{X}})\| \\ \text{s.t.} \quad & |\tilde{\mathbb{X}}| = \tilde{n} \ll n \end{aligned} \tag{1}$$

for a given \tilde{n} , where i.i.d. sampling, distribution compression, or for example clustering, are the potential methods to find $\tilde{\mathbb{X}}$ in an unsupervised manner. We discover a connection between distribution compression and explanation estimation in Propositions 1 & 2.

Proposition 1 (Feature marginalization is bounded by the maximum mean discrepancy between data samples). For two empirical distributions $q_{\mathbb{X}}, q_{\tilde{\mathbb{X}}}$ approximated with a kernel density estimator \mathbf{k} , we have $|f(\mathbf{x}_s; q_{\mathbb{X}}) - f(\mathbf{x}_s; q_{\tilde{\mathbb{X}}})| \leq C_f \cdot \widehat{\text{MMD}}_{\mathbf{k}}(q_{\mathbb{X}}, q_{\tilde{\mathbb{X}}})$, where C_f denotes a constant that bounds the model function f , i.e. $\forall \mathbf{x} \in \mathbb{R}^p, |f(\mathbf{x})| \leq C_f$.

Proposition 1 provides a worst-case bound for feature marginalization, the backbone of local explanations, in terms of the $\text{MMD}_{\mathbf{k}}$ distance between the (often compressed) empirical data distributions. It complements the results for input and model perturbations obtained in (Lin et al., 2023, Lemmas 1 & 4), which also shows how such a bound propagates to the local explanation function g . Effectively, Proposition 1 states that an algorithm minimizing $\text{MMD}_{\mathbf{k}}$, e.g. KT, restricts the approximation error of explanation estimation. This makes CTE a natural contender to improve on i.i.d. sampling, given it was efficient and stable, which we evaluate empirically in extensive experiments.

Compress then explain globally. Local explanations are often aggregated into global explanations based on a representative sample from data, resulting in estimates of feature importance and effects.

Definition 5 (Global explanation). A global explanation is a function that aggregates local explanations g of model f over input samples from distribution $p_{\mathbf{X}}$, i.e. $G(p_{\mathbf{X}}; f, g) := \mathbb{E}_{\mathbf{X} \sim p_{\mathbf{X}}} [g(\mathbf{X}; f, \cdot)]$. For estimation, it uses an empirical distribution $q_{\mathbb{X}}$ in place of $p_{\mathbf{X}}$.

Examples of such global explanations include FEATURE-EFFECTS like partial dependence plots and accumulated local effects (Apley & Zhu, 2020), and SAGE (Covert et al., 2020), which additionally requires as an input labels y of the samples drawn from $p_{\mathbf{X}}$. Notably, the local explanation function g in SAGE itself relies on feature marginalization leading to using $p_{\mathbf{X}}$ twice, i.e. $\mathbb{E}_{\mathbf{X} \sim p_{\mathbf{X}}} [g(\mathbf{X}; f, p_{\mathbf{X}})]$ (see Listing 1 for a practical implementation).

Problem formulation revisited. For global explanations, following Equation 1, we have:

$$\begin{aligned} \min_{\tilde{\mathbf{X}}} \quad & \|G(q_{\tilde{\mathbf{X}}}; f, g) - G(q_{\mathbf{X}}; f, g)\| \\ \text{s.t.} \quad & |\tilde{\mathbf{X}}| = \tilde{n} \ll n. \end{aligned} \quad (2)$$

In Proposition 2, we conduct a worst-case analysis for global aggregated explanations.

Proposition 2 (Global explanation is bounded by the maximum mean discrepancy between data samples). *For two empirical distributions $q_{\mathbf{X}}, q_{\tilde{\mathbf{X}}}$ approximated with a kernel density estimator \mathbf{k} , we have $\|G(q_{\mathbf{X}}; f, g) - G(q_{\tilde{\mathbf{X}}}; f, g)\|_2 \leq C_g \cdot \widehat{\text{MMD}}_{\mathbf{k}}(q_{\mathbf{X}}, q_{\tilde{\mathbf{X}}})$, where C_g denotes a constant that bounds the local explanation function g , i.e. $\forall \mathbf{x} \in \mathbb{R}^p \|g(\mathbf{x}; \cdot)\|_2 \leq C_g$.*

Analogously to Proposition 1, Proposition 2 states that an algorithm minimizing $\text{MMD}_{\mathbf{k}}$, e.g. KT, restricts the approximation error of explanation estimation, which makes CTE a natural contender to improve on i.i.d. sampling. It extends the bounds for total variation distance obtained in (Baniecki et al., 2024). Moreover, in Section 4.5, we explore empirically the impact that minimizing $\text{MMD}_{\mathbf{k}}$ has on decreasing alternative distribution discrepancies in practical (explainable) machine learning settings. It gives further intuition as to why clustering often leads to higher errors in explanation estimation. Our insights may guide future work on tighter theoretical guarantees for improving explanation estimation with distribution compression.

Implementation. The pivotal strength of CTE is that it is simple to plug into the current workflows for explanation estimation as shown in Listing 1 for SAGE. We provide analogous code listings for SHAP, EXPECTED-GRADIENTS and FEATURE-EFFECTS in Appendix C.

```
X, y, model = ...
from goodpoints import compress
ids = compress.compresspp_kt(X, kernel_type="gaussian", g=4)
X_compressed = X[ids]
import sage
imputer = sage.MarginalImputer(model.predict, X_compressed)
estimator = sage.KernelEstimator(imputer)
explanation = estimator(X, y)
# or even
y_compressed = y[ids]
explanation = estimator(X_compressed, y_compressed)
```

Listing 1: Code snippet showing the 3-line plug-in of distribution compression for SAGE estimation.

4 EXPERIMENTS

In experiments, we empirically validate that the CTE paradigm improves explanation estimation across 4 methods, 2 model classes, and over 50 datasets. We compare CTE to the widely adopted practice of i.i.d. sampling (see Appendix A for further motivation). We also report sanity check results for a more deterministic baseline – sampling with k-medoids – where centroids from the clustering define a coreset from the dataset. We use the default hyperparameters of explanation algorithms (details are provided in Appendix D.1). For distribution compression, we use COMPRESS++ implemented in the goodpoints Python package (Dwivedi & Mackey, 2021), where we follow (Shetty et al., 2022) to use a Gaussian kernel \mathbf{k} with $\sigma = \sqrt{2d}$. For all the compared methods, the subsampled set of points is of size \sqrt{n} as we leave oversampling distribution compression for future work. We repeat all experiments where we apply some form of downsampling before explanation estimation 33 times and report the mean and standard error (se.) or deviation (sd.) of metric values.

Ground truth. The goal of CTE is to improve explanation estimation over the standard i.i.d. sampling. We measure the accuracy and effectiveness of explanation estimation with respect to a “ground truth”

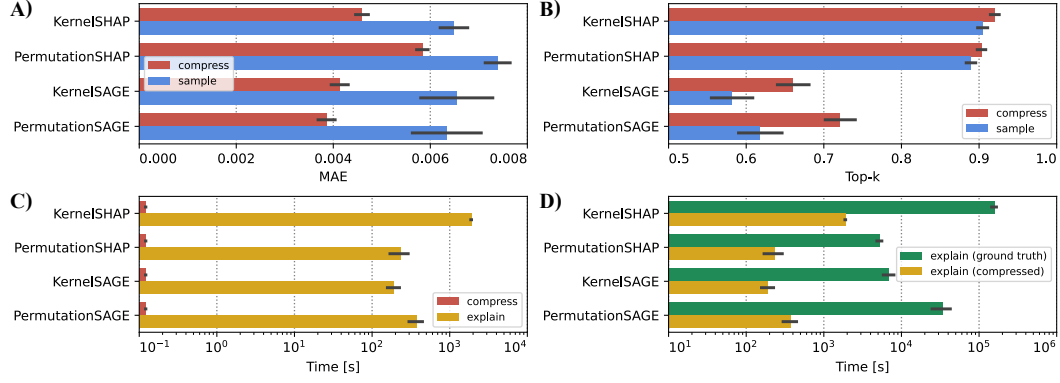


Figure 2: Comparison between CTE and i.i.d. sampling for the two estimators of SHAP and SAGE explanations on the `adult` dataset. **A)** We measure mean absolute error (MAE \downarrow) between feature attribution and importance values, and **B)** the precision in correctly identifying the 5 most important features (Top-k \uparrow). **C)** Comparison between the computational time of distribution compression and explanation estimation on the compressed sample, assuming the time of i.i.d. sampling is 0. **D)** Comparison between the computational time of explanation estimation on the compressed sample and on full data (in green). Analogous results for the other 4 datasets are in Appendix E. (mean \pm se.)

explanation (cf. Appendix I) that is *estimated using a full validation dataset* \mathbb{X} , i.e. without sampling or compression. We consider settings where this is very inefficient to compute in practice ($n := n_{\text{valid}}$ is between 1000 and 25000 samples). For large datasets, we truncate the validation dataset to $20\times$ the size of the compressed dataset. Since some explanation methods include a random component in the algorithm, we repeat their ground truth estimation 3 times and average the resulting explanations.

Accuracy. We are mainly interested in the accuracy of estimating a single explanation, measured by the explanation approximation error. Namely, mean absolute error (MAE), where we measure $\frac{1}{n_{\text{valid}} \cdot d} \sum_{i=1}^{n_{\text{valid}}} \|g(\mathbf{x}^{(i)}; f, q_{\mathbb{X}}) - g(\mathbf{x}^{(i)}; f, q_{\mathbb{X}}^{\text{CTE}})\|_1$ for SHAP and EXPECTED-GRADIENTS, and $\frac{1}{d_G} \|G(q_{\mathbb{X}}; f, g) - G(q_{\mathbb{X}}^{\text{CTE}}; f, g)\|_1$ with $d_G = d$ for SAGE. We have $d_G = 100 \cdot (d + d^2)$ for FEATURE-EFFECTS, since we use 100 uniformly distributed grid points for 1-dimensional effects and 10×10 uniformly distributed grid points for 2-dimensional effects (see Appendix D). For broader context, in Section 4.1, we also measure the precision of correctly indicating the top k features.

Efficiency. We measure the efficiency of compression and explanation estimation with CPU wall-clock time (in seconds), assuming the time of i.i.d. sampling is 0. We rely on popular open-source implementations of the algorithms (see Appendix C) and perform efficiency experiments on a personal computer with an M3 chip. This is to imitate the most standard workflow of explanation estimation, while we acknowledge that specific time estimates will vary in more sophisticated settings.

4.1 CTE IMPROVES THE ACCURACY OF ESTIMATING FEATURE ATTRIBUTIONS & IMPORTANCE

We use the preprocessed datasets and pretrained neural network models from the well-established OpenXAI benchmark (Agarwal et al., 2022). We filter out three datasets with less than 1000 observations in the validation set, where sampling is not crucial, which results in five tasks: `adult` ($n_{\text{valid}} = 9045$, $d = 13$), `compas` ($n_{\text{valid}} = 1235$, $d = 7$), `gaussian` (a synthetic dataset, $n_{\text{valid}} = 1250$, $d = 20$), `gmsc` (Give Me Some Credit, $n_{\text{valid}} = 20442$, $d = 10$), and `heloc` (aka FICO, $n_{\text{valid}} = 1975$, $d = 23$). Further details on datasets and models are provided in Appendix D.2.

We aim to show that CTE improves the estimation of feature attribution and importance explanations, namely for SHAP and SAGE. We experiment with two model-agnostic estimators: kernel-based and permutation-based. For example, Figure 2 shows the differences in MAE and Top-k between CTE and standard i.i.d. sampling on the `adult` dataset. Analogous results for the other 4 datasets from OpenXAI are shown in Appendix E. On all the considered tasks, CTE results in a notable decrease in approximation error when compared to i.i.d. sampling and an increase in precision (for top- k feature identification) with negligible computational overhead. Moreover, CTE results in explanation estimates of significantly smaller variance on average as shown in Table 1.

Table 1: We report the improvement in the mean absolute error of estimating four popular explanations on five datasets from the OpenXAI benchmark. CTE not only improves the accuracy over i.i.d. by 20–45%, but also leads to more stable estimates by about 50%. MAE (\downarrow , \pm sd.) values are scaled and rounded to improve readability while detailed and extended results are reported in Appendix E.

Task	Explanation estimator			
	KERNEL-SHAP	PERMUTATION-SHAP	KERNEL-SAGE	PERMUTATION-SAGE
adult	(i.i.d. $\xrightarrow{\text{diff.}}$ CTE)	73 \pm 14 $\xrightarrow{21\%}$ 58 \pm 6	65 \pm 42 $\xrightarrow{37\%}$ 41 \pm 10	63 \pm 40 $\xrightarrow{40\%}$ 38 \pm 10
compas	10 \pm 4 $\xrightarrow{40\%}$ 6 \pm 2	11 \pm 4 $\xrightarrow{45\%}$ 6 \pm 2	29 \pm 17 $\xrightarrow{38\%}$ 18 \pm 9	28 \pm 16 $\xrightarrow{39\%}$ 17 \pm 8
gaussian	13 \pm 2 $\xrightarrow{38\%}$ 8 \pm 1	15 \pm 2 $\xrightarrow{27\%}$ 11 \pm 1	52 \pm 27 $\xrightarrow{42\%}$ 30 \pm 7	52 \pm 26 $\xrightarrow{44\%}$ 29 \pm 7
gmsc	23 \pm 6 $\xrightarrow{39\%}$ 14 \pm 3	25 \pm 5 $\xrightarrow{32\%}$ 17 \pm 3	30 \pm 13 $\xrightarrow{40\%}$ 18 \pm 5	28 \pm 14 $\xrightarrow{43\%}$ 16 \pm 5
heloc	67 \pm 15 $\xrightarrow{39\%}$ 41 \pm 7	72 \pm 13 $\xrightarrow{33\%}$ 48 \pm 6	34 \pm 10 $\xrightarrow{21\%}$ 27 \pm 6	29 \pm 11 $\xrightarrow{28\%}$ 21 \pm 6

4.2 CTE AS AN EFFICIENT ALTERNATIVE TO I.I.D. SAMPLING IN EXPLANATION ESTIMATION

We find CTE to be a very efficient alternative to standard i.i.d. sampling in explanation estimation. For example, compressing a distribution from 1k to 32 samples takes less than 0.1 seconds, and from 20k to 128 samples takes less than 1 second. The exact runtime will, of course, differ based on the number of features. Figure 3 reports the wall-clock time for datasets of different sizes. Note that the potential runtimes for distribution compression are of magnitudes smaller than the typical runtime of explanation estimation. For example, estimating KERNEL-SHAP for 9k samples using 128 background samples takes 30 minutes, which is about $60\times$ less than estimating the ground truth explanation (Figure 2). Moreover, estimating KERNEL-SHAP or PERMUTATION-SAGE for 1k samples using 32 background samples takes about 10 seconds, which is about $30\times$ less than estimating the ground truth explanation (Appendix E).

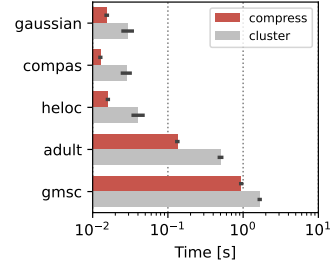


Figure 3: Compressing a distribution from 20k to 128 samples takes less than 1 second to compute on a CPU. (mean \pm se.)

4.3 CTE IMPROVES GRADIENT-BASED EXPLANATIONS SPECIFIC TO NEURAL NETWORKS

Next, we aim to show the broader applicability of CTE by evaluating it on gradient-based explanations specific to neural networks, often fitted to larger unstructured datasets.

Sanity check. We first compress the validation sets of IMDB and ImageNet-1k on a single CPU as a sanity check for the viability of CTE in settings considering larger datasets. For the IMDB dataset ($n_{\text{valid}} = 25000$, $d = 768$), CTE takes as an input text embeddings from the pretrained DistilBERT model’s last layer (preceding a classifier) that has a dimension of size 768. Similarly, for ImageNet-1k ($n_{\text{valid}} = 50000$, $d = 512$), CTE operates on the hidden representation extracted from ResNet-18. Figure 4 shows the optimized MMD_k metric between the distributions and computation time in seconds. We can see that proper compression results in huge benefits w.r.t. MMD_k (compared to i.i.d. sampling and clustering) and only negligible computational overhead.

Accuracy and efficiency. We now study CTE together with EXPECTED-GRADIENTS of neural network models trained to 18 datasets ($n_{\text{valid}} > 1000$, $d \geq 32$) from the OpenML-CC18 (Bischl et al., 2021) and OpenML-CTR23 (Fischer et al., 2023) benchmark suites. Details on datasets and models are provided in Appendix D.2.

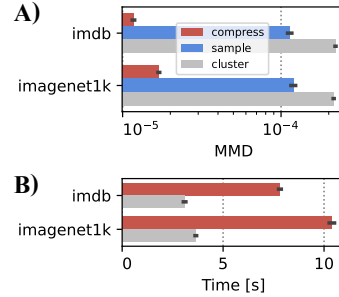


Figure 4: A) COMPRESS++ effectively optimizes MMD_k on unstructured IMDB and ImageNet-1k datasets. B) Compressing a distribution from 25k–50k to 128 samples in 512–768 dimensions takes about 5–10 sec. to compute on a CPU. (mean \pm se.)

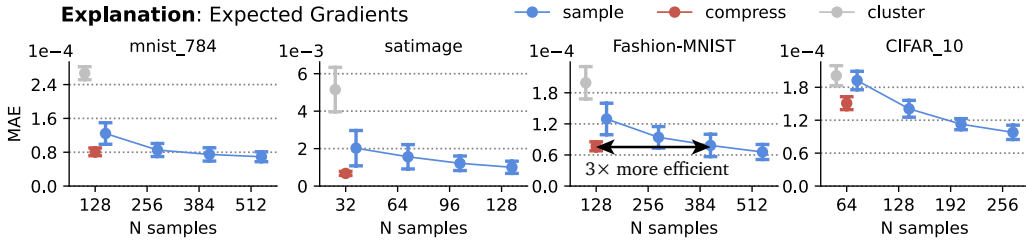


Figure 5: Comparison between CTE, i.i.d. sampling and clustering for EXPECTED-GRADIENTS explanations on the 4 image classification datasets. We measure mean absolute error (MAE \downarrow) between feature attribution values. CTE is not only more accurate but also more stable as measured with deviation. Analogous results for the remaining 14 datasets are in Appendix F. (mean \pm sd.)

In Figure 5, we show the explanation approximation error for 4 image classification tasks, while analogous results for the remaining 14 datasets are provided in Appendix F. Additionally here, we vary the number of data points sampled from i.i.d. to inspect the increase in efficiency of CTE. In all cases, CTE achieves on-par approximation error using fewer samples than i.i.d. sampling, i.e. requiring fewer model inferences, resulting in faster computation and saved resources. The accuracy improvements are significant, i.e. CTE decreases the estimation error for EXPECTED-GRADIENTS by 35% on `mnist_784` (Welch’s t-test: $p < 1e-10$), by 40% on `Fashion-MNIST` ($p < 1e-10$), and by 21% on `CIFAR_10` ($p < 1e-10$). Moreover, CTE provides 2–3 \times efficiency improvements as measured by the number of samples required for i.i.d. to reach the error of CTE.

Model-agnostic explanation of a language model. In Appendix F, we further experiment with applying CTE to improve the estimation of G-LIME (Li et al., 2023) explaining the predictions of a DistilBERT language model trained on the IMDB dataset for sentiment analysis.

4.4 ABLATIONS WITH ANOTHER 30 DATASETS, AN XGBOOST MODEL & FEATURE EFFECTS

For a convincing case to use CTE instead of i.i.d. in practice, we perform additional empirical analysis on various datasets, with a different model class, and include another global explanation method. More specifically, we use CTE to improve FEATURE-EFFECTS of XGBoost models trained on further 30 datasets ($n_{\text{valid}} > 1000$, $d < 32$) from OpenML-CC18 and OpenML-CTR23. Details on datasets and models are provided in Appendix D.2. Moreover, we include SHAP and SAGE in the benchmark similarly to Section 4.1. As another ablation, SAGE is evaluated in two variants that consider either compressing only the background data (a rather typical scenario), or using the compressed samples as both background and foreground data (as indicated with “fg.”; refer to Listing 1 for this distinction).

Figure 6 shows the explanation approximation error for 3 predictive tasks, while analogous results for the remaining explanation estimators and 27 datasets are provided in Appendix G. We observe that CTE significantly improves the estimation of FEATURE-EFFECTS in all cases. We further confirm the conclusions from Sections 4.1 & 4.2 that CTE improves SHAP and SAGE. Another insight is that, on average, CTE provides a smaller improvement over i.i.d. sampling when considering compressing foreground data in SAGE.

Conclusion from the experiments. In Figure 7, we aggregated the results from Sections 4.3 & 4.4 to conclude the main claim that CTE offers 2–3 \times improvements in efficiency over i.i.d. sampling.

4.5 KERNEL THINNING ON DATASETS FOR (EXPLAINABLE) MACHINE LEARNING

We have already established that distribution compression is a viable approach to data sampling, which regularly entails a better approximation of explanations. Moreover, its computational overhead is negligible when applied before explanation estimation. To provide more context on discovering the theoretical justification for CTE from Section 3, we aim to show that COMPRESS++ entails a better approximation of feature distribution on popular datasets for (explainable) machine learning. This is out-of-the-box, without tuning its hyperparameters, which is a natural direction for future work.

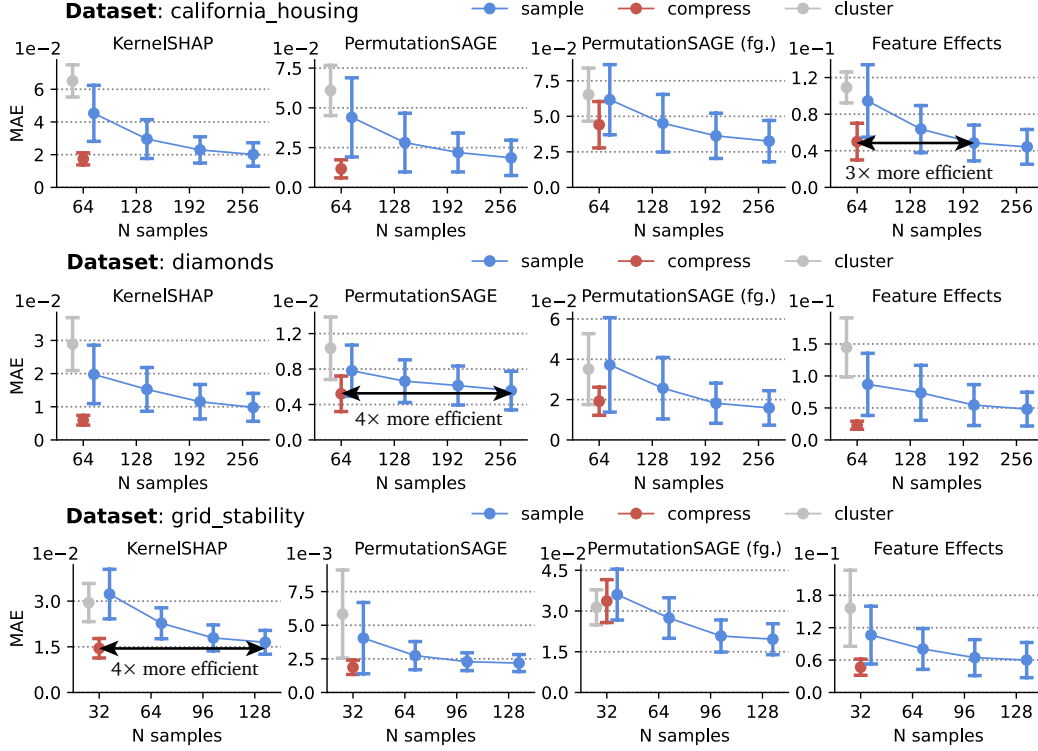


Figure 6: CTE improves the approximation error of local and global removal-based explanations. SAGE is evaluated in two variants that consider either compressing only the background data (default), or using the compressed samples as both background and foreground data (as indicated with “fg.”). Analogous results for the remaining estimators and 27 datasets are in Appendix G. (mean \pm sd.)

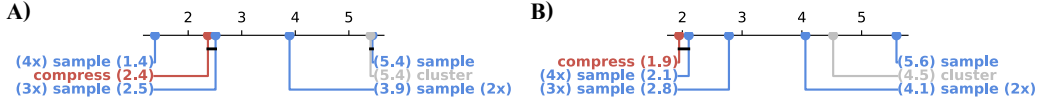


Figure 7: Critical difference diagrams of average ranks (lower is better) aggregated over 6 explanation estimators and 48 dataset-model pairs: **A)** for MAE averaged over repeats, and **B)** for the sd. of MAE over repeats that corresponds to the stability of explanation estimation. CTE often achieves on-par explanation approximation error using 2–3 \times fewer samples, i.e. requiring 2–3 \times fewer model inferences, which is efficient. Moreover, CTE guarantees more stable estimates than i.i.d. sampling.

Measuring distribution change. In general, measuring the similarity of distributions or datasets is challenging, and many metrics with various properties have been proposed for this task (Gibbs & Su, 2002). Here, we report the following distance metric values between the original and compressed distribution: the optimized MMD_k, total variation distance (TV, Gibbs & Su, 2002), Kullback–Leibler divergence (KL, Gibbs & Su, 2002), and d-dimensional Wasserstein distance (WD, Feydy et al., 2019; Laberge et al., 2023). Since approximating d-dimensional TV and KL is infeasible in practice (see e.g. Sriperumbudur et al., 2012, section 5), we report an average of the top-3 largest discrepancies between the 1-dimensional distributions of features as a proxy.

Result. In Figure 8, we observe that COMPRESS++ works much better in terms of MMD_k on all five datasets from OpenXAI, compared to standard i.i.d. sampling or the clustering baseline, which is no surprise as this metric is internally optimized by the former. Note that it also leads to notable improvements in all other metrics. Overall, there is no consistent improvement in approximating the distribution using clustering, which explains why it leads to higher error in explanation estimation.

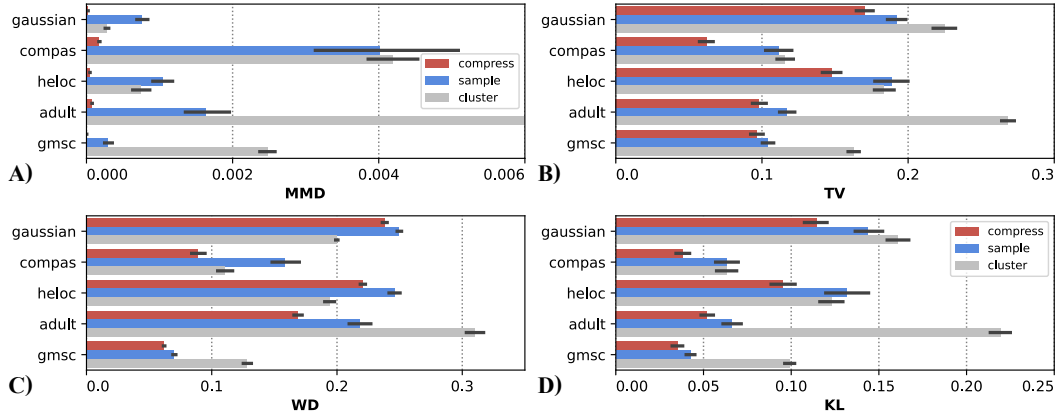


Figure 8: COMPRESS++ with Gaussian kernel on five datasets (rows) for the four considered distribution change metrics (panels): **A)** MMD_k , **B)** total variation distance, **C)** d-dimensional Wasserstein distance, and **D)** Kullback–Leibler divergence. The length of the bar is the mean value \pm standard error across statistical repetitions, where color indicates the applied downsampling method.

5 DISCUSSION

We propose *compress then explain* as a powerful alternative to the conventional *sample then explain* paradigm in explanation estimation. CTE has the potential to improve approximation error across a wide range of explanation methods for various predictive tasks. Specifically, we show accuracy and stability improvements in popular removal-based explanations that marginalize feature influence, and in general, global explanations that aggregate local explanations over a subset of data. Moreover, CTE leads to more efficient explanation estimation by decreasing the computational resources (time, model inferences) required to achieve error on par with a larger i.i.d. sample size.

Future work on methods for marginal distribution compression other than kernel thinning and clustering will bring further improvements in the performance of explanation estimation. Distribution compression methods, by design, have hyperparameters that may impact the empirical results. Although we have shown that the default COMPRESS++ algorithm is a robust baseline, exploring the tunability of its hyperparameters is a natural future work direction (similarly as in the case of conditional sampling methods, Olsen et al., 2024). We used the Gaussian kernel because it is the standard in the field of distribution compression (Dwivedi & Mackey, 2022; Shetty et al., 2022; Domingo-Enrich et al., 2023), especially in experimental analysis, and is generally adopted within machine learning applications. Although our empirical validation shows that the Gaussian kernel works well for over 50 datasets, exploring other kernels for which theoretical thinning error bounds exist, like Matérn or B-spline (Dwivedi & Mackey, 2021), is a viable future work direction. Furthermore, especially for tabular datasets, dealing with categorical features can be an issue, which we elaborate on in Appendix D.2. Specifically for supervised learning, a stratified variant of kernel thinning taking into account a distribution of the target feature could further improve loss-based explanations like SAGE, or even the estimation of group fairness metrics. In concurrent work, Gong et al. (2024) generalize KT to speed up supervised learning problems involving kernel methods. One could also investigate how influence functions (Koh & Liang, 2017), which aim to attribute the importance of data to the model’s prediction, can guide sampling for efficient explanation estimation.

Broader impact. In general, improving explanation methods has positive implications for humans interacting with AI systems (Rong et al., 2024). But, specifically in the context of this work, biased sampling can be exploited to manipulate the explanation results (Slack et al., 2020; Baniecki & Biecek, 2022; Laberge et al., 2023). CTE could minimize the risk of such adversaries and prevent “random seed/state hacking” based on the rather unstable i.i.d. sampling from data in empirical research (Herrmann et al., 2024).

Code. We provide additional details on reproducibility in the Appendix, as well as the code to reproduce all experiments in this paper is available at <https://github.com/hbaniecki/compress-then-explain>.

ACKNOWLEDGMENTS

This work was financially supported by the Polish National Science Centre grant number 2021/43/O/ST6/00347, and carried out with the support of the Laboratory of Bioinformatics and Computational Genomics and the High Performance Computing Center of the Faculty of Mathematics and Information Science, Warsaw University of Technology. Hubert Baniecki gratefully acknowledges scholarship funding from the Polish National Agency for Academic Exchange under the Preludium Bis NAWA 3 program. We want to thank Maximilian Muschalik, Mateusz Biesiadowski, Paulina Kaczynska, Anna Semik, and anonymous reviewers for their valuable feedback regarding this work.

REFERENCES

- Kjersti Aas, Martin Jullum, and Anders Løland. Explaining individual predictions when features are dependent: More accurate approximations to Shapley values. *Artificial Intelligence*, 298:103502, 2021. [1](#), [2.1](#)
- Chirag Agarwal, Satyapriya Krishna, Eshika Saxena, Martin Pawelczyk, Nari Johnson, Isha Puri, Marinka Zitnik, and Himabindu Lakkaraju. OpenXAI: Towards a transparent evaluation of model explanations. In *NeurIPS*, 2022. [4.1](#), [D.2](#)
- Pankaj K. Agarwal, Sarel Har-Peled, and Kasturi R. Varadarajan. Approximating extent measures of points. *Journal of the ACM*, 51(4):606–635, 2004. [1](#)
- Daniel W. Apley and Jingyu Zhu. Visualizing the effects of predictor variables in black box supervised learning models. *Journal of the Royal Statistical Society: Series B (Statistical Methodology)*, 82(4):1059–1086, 2020. [1](#), [2.1](#), [3](#), [D.1](#)
- Hubert Baniecki and Przemyslaw Biecek. Manipulating SHAP via Adversarial Data Perturbations (Student Abstract). In *AAAI*, 2022. [5](#)
- Hubert Baniecki, Giuseppe Casalicchio, Bernd Bischl, and Przemyslaw Biecek. On the Robustness of Global Feature Effect Explanations. In *ECML PKDD*, 2024. [3](#)
- Bernd Bischl, Giuseppe Casalicchio, Matthias Feurer, Pieter Gijsbers, Frank Hutter, Michel Lang, Rafael Gomes Mantovani, Jan N. van Rijn, and Joaquin Vanschoren. OpenML benchmarking suites. In *NeurIPS*, 2021. [4.3](#), [D.2](#)
- Hugh Chen, Ian C Covert, Scott M Lundberg, and Su-In Lee. Algorithms to estimate Shapley value feature attributions. *Nature Machine Intelligence*, 5(6):590–601, 2023. [1](#)
- Jianbo Chen, Le Song, Martin J. Wainwright, and Michael I. Jordan. Learning to explain: An information-theoretic perspective on model interpretation. In *ICML*, 2018. [1](#), [1](#), [2.1](#)
- Ruoyu Chen, Hua Zhang, Siyuan Liang, Jingzhi Li, and Xiaochun Cao. Less is more: Fewer interpretable region via submodular subset selection. In *ICLR*, 2024. [1](#)
- Zhaozheng Chen and Qianru Sun. Extracting class activation maps from non-discriminative features as well. In *CVPR*, 2023. [A](#)
- Badr-Eddine Chérif-Abdellatif and Pierre Alquier. Finite sample properties of parametric mmd estimation: Robustness to misspecification and dependence. *Bernoulli*, 28(1), 2022. [2.2](#)
- A. Feder Cooper, Wentao Guo, Khiem Pham, Tiancheng Yuan, Charlie F. Ruan, Yucheng Lu, and Christopher De Sa. Coordinating distributed example orders for provably accelerated training. In *NeurIPS*, 2023. [1](#)
- Ian Covert and Su-In Lee. Improving KernelSHAP: Practical Shapley value estimation via linear regression. In *AISTATS*, 2021. [1](#)
- Ian Covert, Scott M Lundberg, and Su-In Lee. Understanding global feature contributions with additive importance measures. In *NeurIPS*, 2020. [1](#), [2.1](#), [3](#), [A](#), [D.1](#)

- Ian Covert, Scott Lundberg, and Su-In Lee. Explaining by removing: A unified framework for model explanation. *Journal of Machine Learning Research*, 22(209):1–90, 2021. [1](#), [2.1](#)
- Carles Domingo-Enrich, Raaz Dwivedi, and Lester Mackey. Compress then test: Powerful kernel testing in near-linear time. In *AISTATS*, 2023. [1](#), [2.2](#), [5](#)
- Jon Donnelly, Srikar Katta, Cynthia Rudin, and Edward Browne. The Rashomon importance distribution: Getting RID of unstable, single model-based variable importance. In *NeurIPS*, 2023. [1](#)
- Raaz Dwivedi and Lester Mackey. Kernel thinning. In *COLT*, 2021. [1](#), [1](#), [2.2](#), [2](#), [4](#), [5](#), [C](#)
- Raaz Dwivedi and Lester Mackey. Generalized kernel thinning. In *ICLR*, 2022. [1](#), [2.2](#), [5](#)
- Gabriel Erion, Joseph D Janizek, Pascal Sturmfels, Scott M Lundberg, and Su-In Lee. Improving performance of deep learning models with axiomatic attribution priors and expected gradients. *Nature Machine Intelligence*, 3(7):620–631, 2021. [1](#), [1](#), [2.1](#), [3](#), [A](#)
- Jean Feydy, Thibault Séjourné, François-Xavier Vialard, Shun-ichi Amari, Alain Trounev, and Gabriel Peyré. Interpolating between optimal transport and MMD using sinkhorn divergences. In *AISTATS*, 2019. [4.5](#)
- Sebastian Felix Fischer, Matthias Feurer, and Bernd Bischl. OpenML-CTR23 – a curated tabular regression benchmarking suite. In *AutoML*, 2023. [4.3](#), [D.2](#)
- Fabian Fumagalli, Maximilian Muschalik, Patrick Kolpaczki, Eyke Hüllermeier, and Barbara Hammer. SHAP-IQ: Unified approximation of any-order Shapley interactions. In *NeurIPS*, 2023. [1](#), [1](#), [2.1](#)
- Sahra Ghalebikesabi, Lucile Ter-Minassian, Karla DiazOrdaz, and Chris C Holmes. On locality of local explanation models. In *NeurIPS*, 2021. [1](#), [1](#), [A](#)
- Alison L Gibbs and Francis Edward Su. On choosing and bounding probability metrics. *International Statistical Review*, 70(3):419–435, 2002. [4.5](#)
- Albert Gong, Kyuseong Choi, and Raaz Dwivedi. Supervised kernel thinning. In *NeurIPS*, 2024. [5](#)
- Arthur Gretton, Karsten M Borgwardt, Malte J Rasch, Bernhard Schölkopf, and Alexander Smola. A kernel two-sample test. *Journal of Machine Learning Research*, 13(1):723–773, 2012. [2.2](#), [2](#), [3](#), [2.2](#)
- Sariel Har-Peled and Soham Mazumdar. On coresets for k-means and k-median clustering. In *STOC*, 2004. [1](#)
- Peter Hase, Harry Xie, and Mohit Bansal. The out-of-distribution problem in explainability and search methods for feature importance explanations. In *NeurIPS*, 2021. [1](#)
- Moritz Herrmann, F. Julian D. Lange, Katharina Eggensperger, Giuseppe Casalicchio, Marcel Wever, Matthias Feurer, David Rügamer, Eyke Hüllermeier, Anne-Laure Boulesteix, and Bernd Bischl. Position paper: Rethinking empirical research in machine learning: Addressing epistemic and methodological challenges of experimentation. In *ICML*, 2024. [5](#)
- Neil Jethani, Mukund Sudarshan, Ian Connick Covert, Su-In Lee, and Rajesh Ranganath. FastSHAP: Real-time Shapley value estimation. In *ICLR*, 2022. [1](#), [1](#)
- Jang-Hyun Kim, Jinuk Kim, Seong Joon Oh, Sangdoo Yun, Hwanjun Song, Joonhyun Jeong, Jung-Woo Ha, and Hyun Oh Song. Dataset condensation via efficient synthetic-data parameterization. In *ICML*, 2022. [1](#)
- Lukas Klein, Carsten T. Lüth, Udo Schlegel, Till J. Bungert, Mennatallah El-Assady, and Paul F. Jäger. Navigating the maze of explainable AI: A systematic approach to evaluating methods and metrics. In *NeurIPS*, 2024. [2.1](#)
- Pang Wei Koh and Percy Liang. Understanding black-box predictions via influence functions. In *ICML*, 2017. [5](#)

- Narine Kokhlikyan, Vivek Miglani, Miguel Martin, Edward Wang, Bilal Alsallakh, Jonathan Reynolds, Alexander Melnikov, Natalia Kliushkina, Carlos Araya, Siqi Yan, and Orion Reblitz-Richardson. Captum: A unified and generic model interpretability library for PyTorch. *arXiv preprint arXiv:2009.07896*, 2020. [D.1](#)
- Patrick Kolpaczki, Viktor Bengs, Maximilian Muschalik, and Eyke Hüllermeier. Approximating the Shapley value without marginal contributions. In *AAAI*, 2024. [1](#)
- Mateusz Krzyżiński, Mikołaj Spytek, Hubert Baniecki, and Przemysław Biecek. SurvSHAP(t): Time-dependent explanations of machine learning survival models. *Knowledge-Based Systems*, 262:110234, 2023. [2.1](#)
- Gabriel Laberge, Ulrich Aivodji, Satoshi Hara, and Foutse Khomh Mario Marchand. Fooling SHAP with Stealthily Biased Sampling. In *ICLR*, 2023. [1](#), [4.5](#), [5](#), [A](#)
- Jeffrey Li, Vaishnavh Nagarajan, Gregory Plumb, and Ameet Talwalkar. A learning theoretic perspective on local explainability. In *ICLR*, 2021. [1](#)
- Xuhong Li, Haoyi Xiong, Xingjian Li, Xiao Zhang, Ji Liu, Haiyan Jiang, Zeyu Chen, and Dejing Dou. G-LIME: Statistical learning for local interpretations of deep neural networks using global priors. *Artificial Intelligence*, 314:103823, 2023. [1](#), [2.1](#), [4.3](#), [F](#)
- Chris Lin, Ian Covert, and Su-In Lee. On the robustness of removal-based feature attributions. In *NeurIPS*, 2023. [3](#)
- Scott M Lundberg and Su-In Lee. A unified approach to interpreting model predictions. In *NeurIPS*, 2017. [1](#), [2.1](#), [3](#), [A](#), [D.1](#)
- Daniel D Lundstrom, Tianjian Huang, and Meisam Razaviyayn. A rigorous study of integrated gradients method and extensions to internal neuron attributions. In *ICML*, 2022. [1](#), [1](#)
- Julia Moosbauer, Julia Herbinger, Giuseppe Casalicchio, Marius Lindauer, and Bernd Bischl. Explaining hyperparameter optimization via partial dependence plots. In *NeurIPS*, 2021. [1](#), [D.1](#)
- Krikamol Muandet, Kenji Fukumizu, Bharath Sriperumbudur, and Bernhard Schölkopf. Kernel mean embedding of distributions: A review and beyond. *Foundations and Trends in Machine Learning*, 10(1–2):1–141, 2017. [2.2](#), [3](#)
- Maximilian Muschalik, Fabian Fumagalli, Barbara Hammer, and Eyke Hüllermeier. Beyond Tree-SHAP: Efficient computation of any-order Shapley interactions for tree ensembles. In *AAAI*, 2024. [1](#)
- Lars H. B. Olsen, Ingrid K. Glad, Martin Jullum, and Kjersti Aas. Using Shapley values and variational autoencoders to explain predictive models with dependent mixed features. *Journal of Machine Learning Research*, 23(213):1–51, 2022. [1](#), [1](#), [2.1](#)
- Lars Henry Berge Olsen, Ingrid Kristine Glad, Martin Jullum, and Kjersti Aas. A comparative study of methods for estimating model-agnostic Shapley value explanations. *Data Mining and Knowledge Discovery*, pp. 1–48, 2024. [1](#), [2.1](#), [5](#)
- Art B Owen. Statistically efficient thinning of a markov chain sampler. *Journal of Computational and Graphical Statistics*, 26(3):738–744, 2017. [1](#)
- Vitali Petsiuk, Abir Das, and Kate Saenko. RISE: Randomized input sampling for explanation of black-box models. In *BMVC*, 2018. [1](#)
- Marco Tulio Ribeiro, Sameer Singh, and Carlos Guestrin. “Why should I trust you?” Explaining the predictions of any classifier. In *KDD*, 2016. [2.1](#), [F](#)
- Yao Rong, Tobias Leemann, Thai-Trang Nguyen, Lisa Fiedler, Peizhu Qian, Vaibhav Unhelkar, Tina Seidel, Gjergji Kasneci, and Enkelejda Kasneci. Towards human-centered explainable AI: A survey of user studies for model explanations. *IEEE Transactions on Pattern Analysis and Machine Intelligence*, 46(4):2104–2122, 2024. [5](#)

- Christian A Scholbeck, Christoph Molnar, Christian Heumann, Bernd Bischl, and Giuseppe Casalicchio. Sampling, intervention, prediction, aggregation: a generalized framework for model-agnostic interpretations. In *ECML PKDD*, 2020. 1
- Ozan Sener and Silvio Savarese. Active learning for convolutional neural networks: A core-set approach. In *ICLR*, 2018. 1
- Abhishek Shetty, Raaz Dwivedi, and Lester Mackey. Distribution compression in near-linear time. In *ICLR*, 2022. 1, 2.2, 2.2, 4, 5
- Dylan Slack, Sophie Hilgard, Emily Jia, Sameer Singh, and Himabindu Lakkaraju. Fooling LIME and SHAP: Adversarial attacks on post hoc explanation methods. In *AIES*, 2020. 5
- Dylan Slack, Anna Hilgard, Sameer Singh, and Himabindu Lakkaraju. Reliable post hoc explanations: Modeling uncertainty in explainability. In *NeurIPS*, 2021. 1, 1
- Bharath K. Sriperumbudur, Arthur Gretton, Kenji Fukumizu, Bernhard Schölkopf, and Gert R.G. Lanckriet. Hilbert space embeddings and metrics on probability measures. *Journal of Machine Learning Research*, 11(50):1517–1561, 2010. 2.2
- Bharath K Sriperumbudur, Kenji Fukumizu, Arthur Gretton, Bernhard Schölkopf, and Gert RG Lanckriet. On the empirical estimation of integral probability metrics. *Electronic Journal of Statistics*, 6:1550–1599, 2012. 4.5
- Erik Strumbelj and Igor Kononenko. An efficient explanation of individual classifications using game theory. *Journal of Machine Learning Research*, 11:1–18, 2010. 1
- Arnaud Van Looveren and Janis Klaise. Interpretable counterfactual explanations guided by prototypes. In *ECML PKDD*, 2021. A
- Tongzhou Wang, Jun-Yan Zhu, Antonio Torralba, and Alexei A. Efros. Dataset distillation. *arXiv preprint arXiv:1811.10959*, 2018. 1
- Borui Zhang, Wenzhao Zheng, Jie Zhou, and Jiwen Lu. Path choice matters for clear attributions in path methods. In *ICLR*, 2024. 1
- Bo Zhao, Konda Reddy Mopuri, and Hakan Bilen. Dataset condensation with gradient matching. In *ICLR*, 2021. 1
- Nicky Zimmerman, Alessandro Giusti, and Jérôme Guzzi. Resource-aware collaborative monte carlo localization with distribution compression. *arXiv preprint arXiv:2404.02010*, 2024. 1

APPENDIX FOR “EFFICIENT AND ACCURATE EXPLANATION ESTIMATION WITH DISTRIBUTION COMPRESSION”

In Appendix B, we derive proofs for Propositions 1 & 2. Appendix C provides code listings for SHAP, EXPECTED-GRADIENTS and FEATURE-EFFECTS, analogous to Listing 1 for SAGE. Additional details on the experimental setup are provided in Appendix D. Appendices E, F & G report experimental results for the remaining datasets. Appendix H comments on compute resources used for experiments. Appendix I provides exemplary visual comparisons of explanations. The code to reproduce all experiments in this paper is available at <https://github.com/hbaniecki/compress-then-explain>.

A Motivation: standard i.i.d. sampling in explanation estimation	16
B Proofs	17
C Implementing CTE in practice	18
D Experimental setup	19
D.1 Explanation hyperparameters	19
D.2 Details on datasets and models	19
E CTE significantly improves the estimation of feature attributions & importance	21
F CTE improves gradient-based explanations	23
G Ablations	25
H Compute resources	35
I Visual comparison of explanations	36

A MOTIVATION: STANDARD I.I.D. SAMPLING IN EXPLANATION ESTIMATION

We find that i.i.d. sampling from datasets is a heuristic often used (and overlooked) in various estimators of post-hoc explanations. Our work aims to first quantify the approximation error introduced by *sample then explain*, and then propose a method to efficiently reduce it. Below are a few examples from the literature on explainability that motivate the shift to our introduced *compress then explain* paradigm.

In (Laberge et al., 2023), we read “For instance, when a dataset is used to represent a background distribution, explainers in the SHAP library such as the *ExactExplainer* and *TreeExplainer* will subsample this dataset by selecting 100 instances uniformly at random when the size of the dataset exceeds 100.”

In (Chen & Sun, 2023), we read “[Footnote 1.] We use a random subset of samples for each class in the real implementation, to reduce the computation costs of clustering.”

In (Ghalebikesabi et al., 2021), we read “After training a convolutional neural network on the MNIST dataset, we explain digits with the predicted label 8 given a background dataset of 100 images with labels 3 and 8.”, as well as “Feature attributions are sorted by similarity according to a preliminary PCA analysis across a subset of 2000 samples from the Adult Income dataset, using 2000 reference points.”

In (Erion et al., 2021), we read “During training, we let k be the number of samples we draw to compute expected gradients for each mini-batch. and “This expectation-based formulation lends itself to a natural, sampling based approximation method: (1) draw samples of x' from the training dataset [...], (2) compute the value inside the expectation for each sample and (3) average over samples.”

In (Van Looveren & Klaise, 2021), we read “We also need a representative, unlabeled sample of the training dataset.”, and in Algorithms 1 and 2: “A sample $X = \{x_1, \dots, x_n\}$ from training set.”

In (Covert et al., 2020), we read “When calculating feature importance, our sampling approximation for SAGE (Algorithm 1) was run using draws from the marginal distribution. We used a fixed set of 512 background samples for the bank, bike and credit datasets, 128 for MNIST, and all 334 training examples for BRCA.”

In the `shap` Python package (Lundberg & Lee, 2017), there is a warning saying “Using 110 background data samples could cause slower run times. Consider using `shap.sample(data, K)` or `shap.kmeans(data, K)` to summarize the background as K samples.”, and the documentation mentions “For small problems, this background dataset can be the whole training set, but for larger problems consider using a single reference value or using the `kmeans` function to summarize the dataset.”

B PROOFS

Below, we derive proofs for Propositions 1 & 2.

Proposition 1 (Feature marginalization is bounded by the maximum mean discrepancy between data samples). *For two empirical distributions $q_{\mathbb{X}}, q_{\widetilde{\mathbb{X}}}$ approximated with a kernel density estimator \mathbf{k} , we have $|f(\mathbf{x}_s; q_{\mathbb{X}}) - f(\mathbf{x}_s; q_{\widetilde{\mathbb{X}}})| \leq C_f \cdot \widehat{\text{MMD}}_{\mathbf{k}}(q_{\mathbb{X}}, q_{\widetilde{\mathbb{X}}})$, where C_f denotes a constant that bounds the model function f , i.e. $\forall \mathbf{x} \in \mathbb{R}^p |f(\mathbf{x})| \leq C_f$.*

Proof. We derive the following inequality:

$$(f(\mathbf{x}_s; p_{\mathbf{X}_{\bar{s}}}) - f(\mathbf{x}_s; q_{\mathbf{X}_{\bar{s}}}))^2 = (\mathbb{E}_{\mathbf{X}_{\bar{s}} \sim p_{\mathbf{X}_{\bar{s}}}} [f(\mathbf{x}_s, \mathbf{X}_{\bar{s}})] - \mathbb{E}_{\mathbf{X}_{\bar{s}} \sim q_{\mathbf{X}_{\bar{s}}}} [f(\mathbf{x}_s, \mathbf{X}_{\bar{s}})])^2 \quad (3)$$

$$= \left(\int f(\mathbf{x}_s, \mathbf{x}_{\bar{s}}) p_{\mathbf{X}_{\bar{s}}}(\mathbf{x}_{\bar{s}}) d\mathbf{x}_{\bar{s}} - \int f(\mathbf{x}_s, \mathbf{x}_{\bar{s}}) q_{\mathbf{X}_{\bar{s}}}(\mathbf{x}_{\bar{s}}) d\mathbf{x}_{\bar{s}} \right)^2 \quad (4)$$

$$(\text{linearity}) = \left(\int f(\mathbf{x}_s, \mathbf{x}_{\bar{s}}) (p_{\mathbf{X}_{\bar{s}}}(\mathbf{x}_{\bar{s}}) - q_{\mathbf{X}_{\bar{s}}}(\mathbf{x}_{\bar{s}})) d\mathbf{x}_{\bar{s}} \right)^2 \quad (5)$$

$$(\text{Cauchy-Schwarz}) \leq \int (f(\mathbf{x}_s, \mathbf{x}_{\bar{s}}))^2 d\mathbf{x}_{\bar{s}} \int (p_{\mathbf{X}_{\bar{s}}}(\mathbf{x}_{\bar{s}}) - q_{\mathbf{X}_{\bar{s}}}(\mathbf{x}_{\bar{s}}))^2 d\mathbf{x}_{\bar{s}} \quad (6)$$

$$(\text{boundedness}) \leq C_f^2 \cdot \int (p_{\mathbf{X}_{\bar{s}}}(\mathbf{x}_{\bar{s}}) - q_{\mathbf{X}_{\bar{s}}}(\mathbf{x}_{\bar{s}}))^2 d\mathbf{x}_{\bar{s}} \quad (7)$$

$$(\text{Definition 3}) = C_f^2 \cdot \widehat{\text{MMD}}_{\mathbf{k}}^2(p_{\mathbf{X}_{\bar{s}}}, q_{\mathbf{X}_{\bar{s}}}). \quad (8)$$

Substituting with empirical distributions, we have

$$|f(\mathbf{x}_s; q_{\mathbb{X}}) - f(\mathbf{x}_s; q_{\widetilde{\mathbb{X}}})| \leq C_f \cdot \widehat{\text{MMD}}_{\mathbf{k}}(q_{\mathbb{X}}, q_{\widetilde{\mathbb{X}}}). \quad (9)$$

□

Proposition 2 (Global explanation is bounded by the maximum mean discrepancy between data samples). *For two empirical distributions $q_{\mathbb{X}}, q_{\widetilde{\mathbb{X}}}$ approximated with a kernel density estimator \mathbf{k} , we have $\|G(q_{\mathbb{X}}; f, g) - G(q_{\widetilde{\mathbb{X}}}; f, g)\|_2 \leq C_g \cdot \widehat{\text{MMD}}_{\mathbf{k}}(q_{\mathbb{X}}, q_{\widetilde{\mathbb{X}}})$, where C_g denotes a constant that bounds the local explanation function g , i.e. $\forall \mathbf{x} \in \mathbb{R}^p \|g(\mathbf{x}; \cdot)\|_2 \leq C_g$.*

Proof. We derive the following inequality:

$$\|G(p_{\mathbf{X}}; f, g) - G(q_{\mathbf{X}}; f, g)\|_2^2 = \|\mathbb{E}_{\mathbf{X} \sim p_{\mathbf{X}}} [g(\mathbf{X}; f, \cdot)] - \mathbb{E}_{\mathbf{X} \sim q_{\mathbf{X}}} [g(\mathbf{X}; f, \cdot)]\|_2^2 \quad (10)$$

$$= \left\| \int g(\mathbf{x}) p_{\mathbf{X}}(\mathbf{x}) d\mathbf{x} - \int g(\mathbf{x}) q_{\mathbf{X}}(\mathbf{x}) d\mathbf{x} \right\|_2^2 \quad (11)$$

$$(\text{linearity}) = \left\| \int g(\mathbf{x}) (p_{\mathbf{X}}(\mathbf{x}) - q_{\mathbf{X}}(\mathbf{x})) d\mathbf{x} \right\|_2^2 \quad (12)$$

$$(\text{Cauchy-Schwarz}) \leq \int \|g(\mathbf{x})\|_2^2 d\mathbf{x} \int (p_{\mathbf{X}}(\mathbf{x}) - q_{\mathbf{X}}(\mathbf{x}))^2 d\mathbf{x} \quad (13)$$

$$(\text{boundedness}) \leq C_g^2 \cdot \int (p_{\mathbf{X}}(\mathbf{x}) - q_{\mathbf{X}}(\mathbf{x}))^2 d\mathbf{x} \quad (14)$$

$$(\text{Definition 3}) = C_g^2 \cdot \widehat{\text{MMD}}_{\mathbf{k}}^2(p_{\mathbf{X}}, q_{\mathbf{X}}). \quad (15)$$

Substituting with empirical distributions, we have

$$\|G(q_{\mathbb{X}}; f, g) - G(q_{\widetilde{\mathbb{X}}}; f, g)\|_2 \leq C_g \cdot \widehat{\text{MMD}}_{\mathbf{k}}(q_{\mathbb{X}}, q_{\widetilde{\mathbb{X}}}). \quad (16)$$

□

C IMPLEMENTING CTE IN PRACTICE

CTE is simple to plug-into the current workflows for explanation estimation as shown in Listing 1 for SAGE, Listing 2 for SHAP, Listing 3 for EXPECTED-GRADIENTS, and Listing 4 for FEATURE-EFFECTS. We use the `goodpoints` Python package (Dwivedi & Mackey, 2021, MIT license).

```
X, model = ...
from goodpoints import compress
ids = compress.compresspp_kt(X, kernel_type=b"gaussian", g=4)
X_compressed = X[ids]
import shap
masker = shap.maskers.Independent(X_compressed)
explainer = shap.PermutationExplainer(model.predict, masker)
explanation = explainer(X)
```

Listing 2: Code snippet showing the 3-line plug-in of distribution compression for SHAP estimation.

```
X, model = ...
from goodpoints import compress
ids = compress.compresspp_kt(X, kernel_type=b"gaussian", g=4)
X_compressed = X[ids]
import captum
explainer = captum.attr.IntegratedGradients(model)
import torch
inputs = torch.as_tensor(X)
baselines = torch.as_tensor(X_compressed)
explanation = torch.mean(torch.stack([
    explainer.attribute(inputs, baselines[[i]], target=1)
    for i in range(baselines.shape[0])
]), dim=0)
```

Listing 3: Code snippet showing the plug-in of distribution compression for EXPECTED-GRADIENTS.

```
X, model = ...
from goodpoints import compress
ids = compress.compresspp_kt(X, kernel_type=b"gaussian", g=4)
X_compressed = X[ids]
import alibi
explainer = alibi.explainers.PartialDependence(predictor=model.predict)
explanation = explainer.explain(X_compressed)
```

Listing 4: Code snippet showing the plug-in of distribution compression for FEATURE-EFFECTS.

D EXPERIMENTAL SETUP

D.1 EXPLANATION HYPERPARAMETERS

In Section 4, we experiment with 4 explanation methods (6 estimators). Without the loss of generality, in case of classification models, we always explain a prediction for the 2nd class. For SHAP, we use the KERNEL-SHAP and PERMUTATION-SHAP implementations from the `shap` Python package (Lundberg & Lee, 2017, MIT license) with default hyperparameters (notably, `npermutations=10` in the latter). For SAGE, we use the KERNEL-SAGE and PERMUTATION-SAGE implementations from the `sage` Python package (Covert et al., 2020, MIT license). We use default hyperparameters; notably, a cross-entropy loss for classification and mean squared error for regression. For EXPECTED-GRADIENTS, we aggregate with mean the integrated gradients explanations from the `captum` Python package (Kokhlikyan et al., 2020, BSD-3 license), for which we use default hyperparameters; notably, `n_steps=50` and `method="gausslegendre"`. For FEATURE-EFFECTS, we implement the partial dependence algorithm (Apley & Zhu, 2020; Moosbauer et al., 2021) ourselves for maximum computational speed in case of 2-dimensional plots, mimicking the popular open-source implementations.¹ We use 100 uniformly distributed grid points for 1-dimensional plots and 10×10 uniformly distributed grid points for 2-dimensional plots.

D.2 DETAILS ON DATASETS AND MODELS

Table 2 shows details of datasets from the OpenXAI (Agarwal et al., 2022, MIT license) benchmark used in Sections 4.1, 4.2 & 4.5. To each dataset, there is a pretrained neural network with an accuracy of 92% (gaussian), 85% (compas), 74% (heloc), 85% (adult) and 93% (gmisc). We do not further preprocess data; notably, feature values are already scaled to $[0, 1]$.

Table 2: Datasets from OpenXAI with $n_{\text{valid}} > 1000$ used in experiments.

Dataset	n_{train}	n_{valid}	d	No. classes
gaussian	3750	1250	20	2
compas	4937	1235	7	2
heloc	7896	1975	23	2
adult	36177	9045	13	2
gmisc	81767	20442	10	2

Table 3 shows details of datasets from the OpenML-CC18 (Bischl et al., 2021, BSD-3 license) and OpenML-CTR23 (Fischer et al., 2023, BSD-3 license) benchmarks used in Sections 4.3 & 4.4. We first split all datasets in 75:25 (train:validation) ratio and left 48 datasets with $n_{\text{valid}} > 1000$ for our experiments. For the 30 smaller ($d < 32$) datasets, we train an XGBoost model with default hyperparameters (200 estimators) and explain it with SHAP, SAGE, FEATURE-EFFECTS. For the 18 bigger ($d \geq 32$) datasets, we train a 3-layer neural network model with (128, 64) neurons in hidden ReLU layers and explain it with EXPECTED-GRADIENTS. We perform basic preprocessing of data: (1) remove features with a single or n unique values, (2) target encode categorical features, (3) impute missing values with mean, and (4) standardize features.

In general, categorical features can be an issue for clustering and distribution compression algorithms; so are for many explanation algorithms and conditional distribution samplers. Although target encoding worked well in our setup, we envision two additional heuristics to deal with categorical features: (1) perform distribution compression using a dataset restricted to non-categorical features, (2) target encode categorical features only for distribution compression.

¹<https://docs.seldon.io/projects/alibi/en/latest/api/alibi.explainers.html#alibi.explainers.PartialDependence>; <https://interpret.ml/docs/python/api/PartialDependence>

Table 3: Datasets from OpenML-CC18 and OpenML-CTR23 with $n_{\text{valid}} > 1000$ used in experiments.

Dataset	Task ID	n_{train}	n_{valid}	d	No. classes
phoneme	9952	4053	1351	5	2
wilt	146820	3629	1210	5	2
cps88wages	361261	21116	7039	6	—
jungle_chess	167119	33614	11205	6	3
abalone	361234	3132	1045	8	—
electricity	219	33984	11328	8	2
kin8nm	361258	6144	2048	8	—
california_housing	361255	15480	5160	8	—
brazilian_houses	361267	8019	2673	9	—
diamonds	361257	40455	13485	9	—
physiochemical_protein	361241	34297	11433	9	—
white_wine	361249	3673	1225	11	—
health_insurance	361269	16704	5568	11	—
grid_stability	361251	7500	2500	12	—
adult	7592	36631	12211	14	2
naval_propulsion_plant	361247	8950	2984	14	—
miami_housing	361260	10449	3483	15	—
letter	6	15000	5000	16	26
bank-marketing	14965	33908	11303	16	2
pendigits	32	8244	2748	16	10
video_transcoding	361252	51588	17196	18	—
churn	167141	3750	1250	20	2
kings_county	361266	16209	5404	21	—
numera128.6	167120	72240	24080	21	2
sarcos	361254	36699	12234	21	—
cpu_activity	361256	6144	2048	21	—
jm1	3904	8163	2722	21	2
wall-robot-navigation	9960	4092	1364	24	4
fifa	361272	14383	4795	28	—
PhishingWebsites	14952	8291	2764	30	2
pumadyn32nh	361259	6144	2048	32	—
GestureSegmentation	14969	7404	2469	32	5
satimage	2074	4822	1608	36	6
texture	125922	4125	1375	40	11
connect-4	146195	50667	16890	42	3
fps_benchmark	361268	18468	6156	43	—
wave_energy	361253	54000	18000	48	—
theorem-proving	9985	4588	1530	51	6
spambase	43	3450	1151	57	2
optdigits	28	4215	1405	64	10
superconductivity	361242	15947	5316	81	—
nomao	9977	25848	8617	118	2
har	14970	7724	2575	561	6
isolet	3481	5847	1950	617	26
mnist_784	3573	52500	17500	784	10
Fashion-MNIST	146825	52500	17500	784	10
Devnagari-Script	167121	69000	23000	1024	46
CIFAR_10	167124	45000	15000	3072	10

E CTE SIGNIFICANTLY IMPROVES THE ESTIMATION OF FEATURE ATTRIBUTIONS & IMPORTANCE

We report the differences in MAE and Top-k between CTE and i.i.d. sampling in Figure 9 (*compas*), Figure 10 (*heloc*), Figure 11 (*gmsc*) and Figure 12 (*gaussian*). On all the considered tasks, CTE offers a notable decrease in approximation error of SHAP and SAGE with negligible computational overhead (as measured by time in seconds).

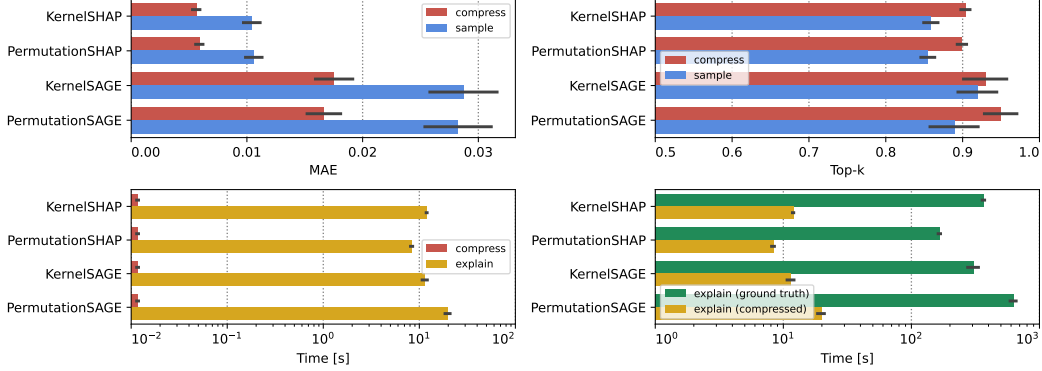


Figure 9: Extended Figure 2 (1/4). CTE improves SHAP and SAGE estimation by using the compressed samples as background data for the *compas* dataset. We measure mean absolute error (MAE \downarrow) between feature attribution and importance values, as well as the precision in correctly indicating the 3 most important features (Top-k \uparrow). Computational resources required to compress a distribution are negligible in the context of explanation estimation. (mean \pm se.)

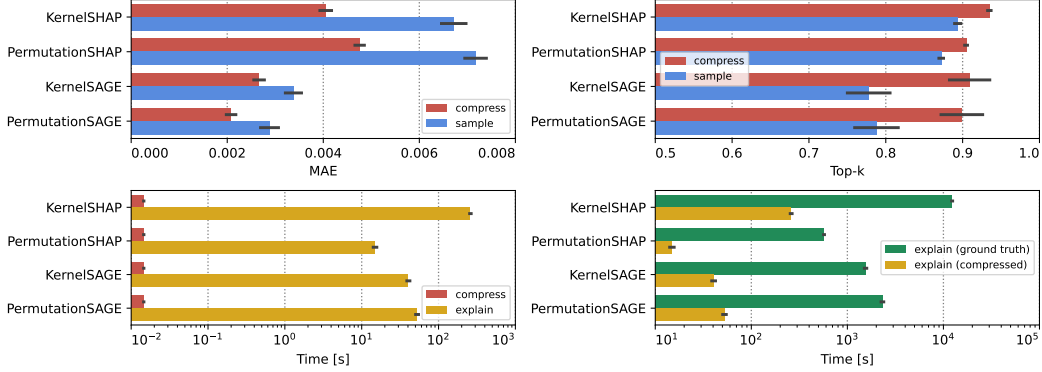


Figure 10: Extended Figure 2 (2/4). CTE improves SHAP and SAGE estimation on the *heloc* dataset.

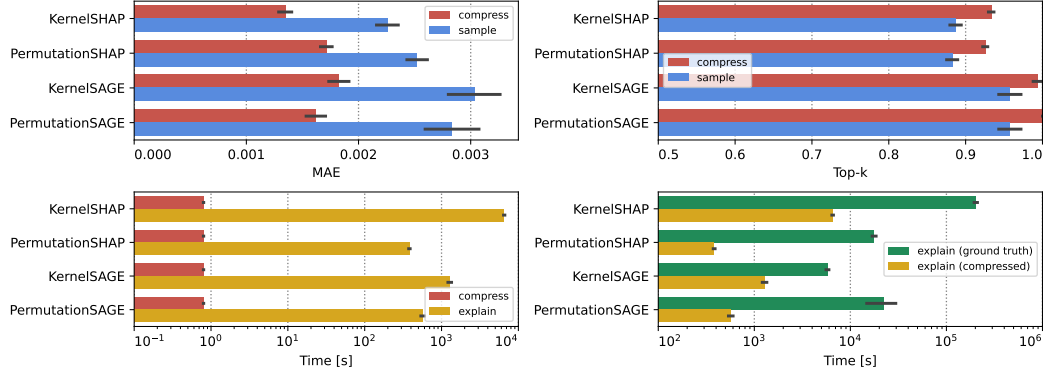


Figure 11: Extended Figure 2 (3/4). CTE improves SHAP and SAGE estimation by using the compressed samples as background data for the `gmsc` dataset. We measure mean absolute error (MAE \downarrow) between feature attribution and importance values, as well as the precision in correctly indicating the 5 most important features (Top-k \uparrow). Computational resources required to compress a distribution are negligible in the context of explanation estimation. (mean \pm se.)

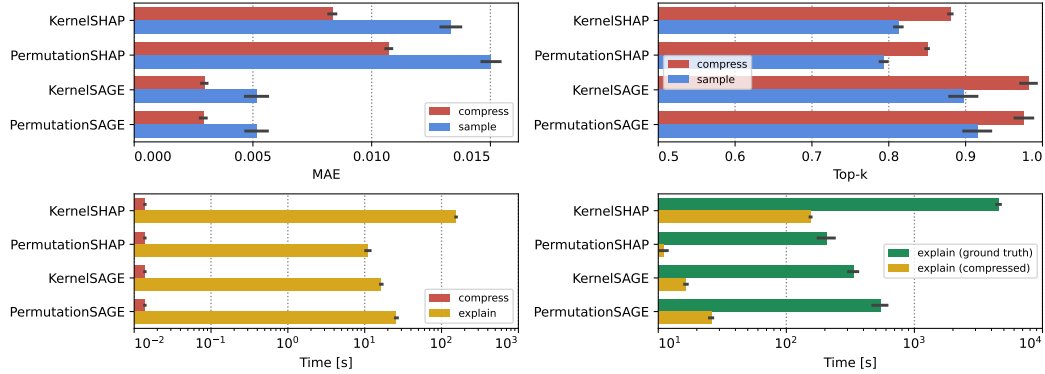


Figure 12: Extended Figure 2 (4/4). CTE improves SHAP and SAGE estimation on the `gaussian` dataset.

F CTE IMPROVES GRADIENT-BASED EXPLANATIONS

Figure 13 shows the EXPECTED-GRADIENTS approximation error for 18 datasets. In all cases, CTE achieves on-par approximation error using fewer samples than i.i.d. sampling, i.e. requiring fewer model inferences, resulting in faster computation and saved resources.

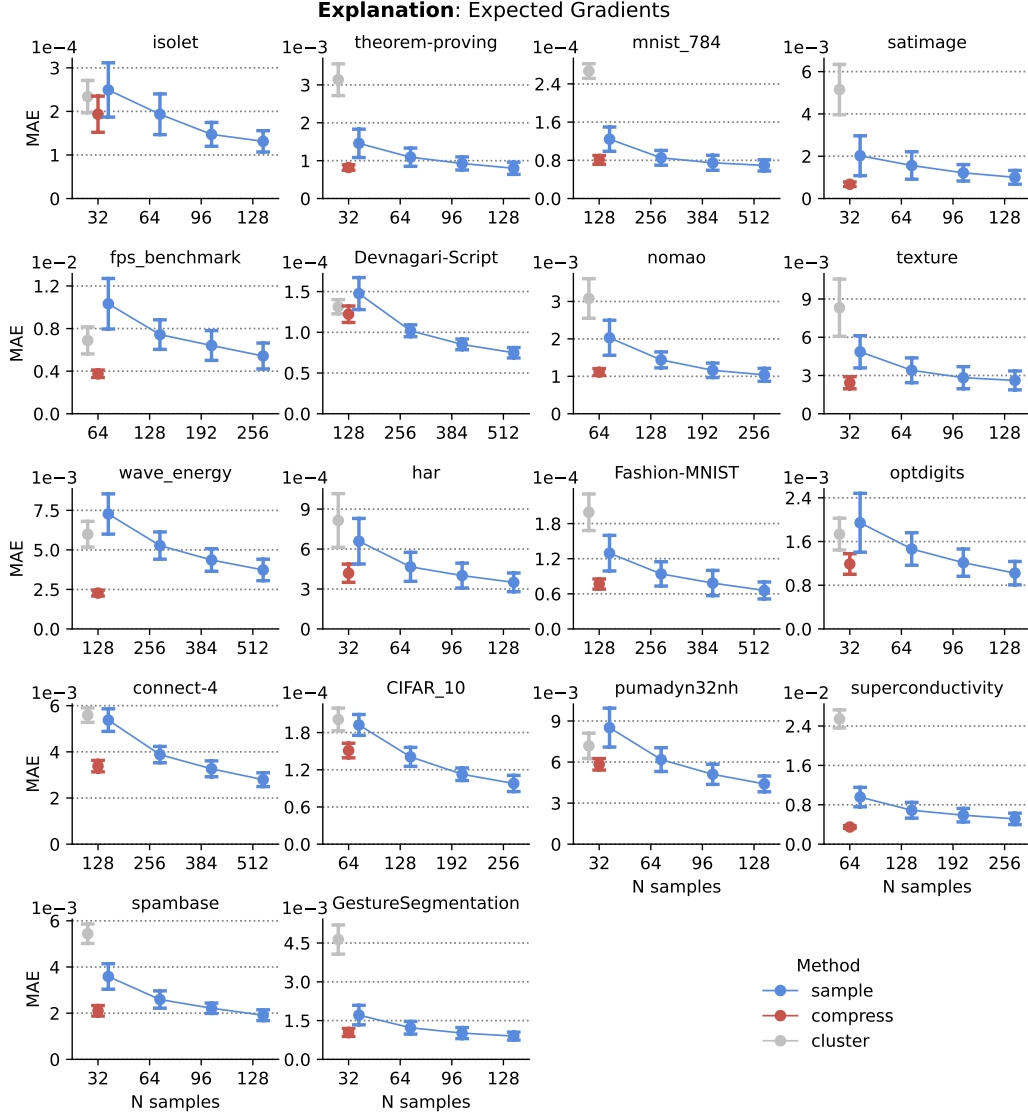


Figure 13: Extended Figure 5. Comparison between CTE, i.i.d. sampling and clustering for EXPECTED-GRADIENTS explanations on 18 datasets. We measure mean absolute error (MAE \downarrow) between feature attribution values. CTE is not only more efficient and accurate, but also more stable as measured with deviation. (mean \pm sd.)

Model-agnostic explanation of a language model. We further experimented with applying CTE to improve the estimation of global aggregated LIME (Ribeiro et al., 2016), aka G-LIME (Li et al., 2023), which is a more complex setup that we leave for future work. We aim to explain the predictions of a DistilBERT language model² trained on the IMDB dataset³ for sentiment analysis. We calculate LIME with $k = 10$ for all samples from the validation set using an A100 GPU and aggregate these local explanations into global token importance with a mean of absolute normalized values (Li et al., 2023), which is the “ground truth” explanation. We then compress the set with i.i.d. sampling, CTE, and clustering based on the inputs’ text embeddings from the model’s last layer (preceding a classifier) that has a dimension of size 768. Figure 14 shows results for explanation approximation error and an exemplary comparison between the explanations relating to Figure 1. To obtain these results, we used $8\times$ more samples than the typical compression scenario (still $25\times$ fewer than the full sample) so as to overcome the issue of rare tokens skewing the results. It becomes challenging to compute the distance between the ground truth and approximated explanations as the latter contains significantly fewer tokens (features), as opposed to previous experiments where these two explanations always had equal dimensions. Thus, MAE becomes biased towards sparse explanations and popular tokens, i.e. an explanation with a single token of well-approximated importance could have an error close to 0. For context, we measure TV between the discrete distributions of tokens in local explanations before the global aggregation (lower is better). We report results for different token cutoffs, where we remove the tokens from the ground truth explanation by their rarity, which saturates at 5% tokens left.

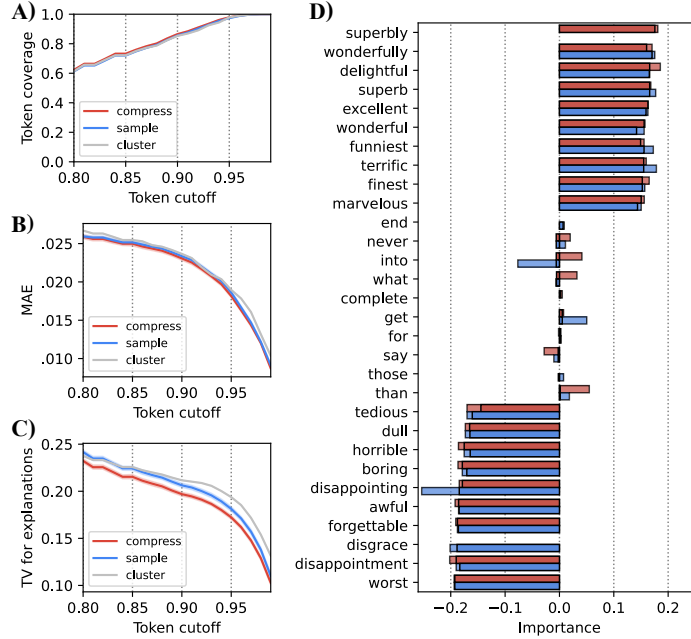


Figure 14: CTE for G-LIME of a DistilBERT model classifying IMDB reviews. **A)** It is not obvious how to measure the distance between global explanations containing different sets of tokens (Token coverage in % w.r.t. ground truth, \uparrow). Therefore, we gradually remove rare tokens from the measurement based on their occurrence in the ground truth explanation (Token cutoff in quantiles). **B)** Measurement of mean absolute error (MAE, \downarrow) between aggregated global explanations. **C)** Measurement of total variation distance (TV, \downarrow) between token occurrences in local explanations before global aggregation. **D)** We show an exemplary “worst-case” explanation, i.e. with the lowest MAE for cutoff 0.95 where token coverage is over 99%, for both CTE and i.i.d. sampling. For this visualization, we only show the importance of the 5 most positive/negative tokens, and 5 tokens with the importance closest to zero. Explanation approximation error is indicated with transparent bars. Notably, i.i.d. sampling misses containing any input with an important token “superbly”, while CTE misses “disgrace”. Sampling overestimates the global importance of tokens “disappointing”, “into” and “get”, while CTE, for example, overestimates “than” and underestimates “tedious” or “delightful”.

²<https://huggingface.co/dfurman/distilbert-base-uncased-imdb>

³<https://huggingface.co/datasets/stanfordnlp/imdb>

G ABLATIONS

Figures 15–23 report the explanation approximation error for 30 predictive tasks. We observe that CTE significantly improves the estimation of FEATURE-EFFECTS in all cases. Another insight is that, on average, CTE provides a smaller improvement over i.i.d. sampling when considering compressing foreground data in SAGE.

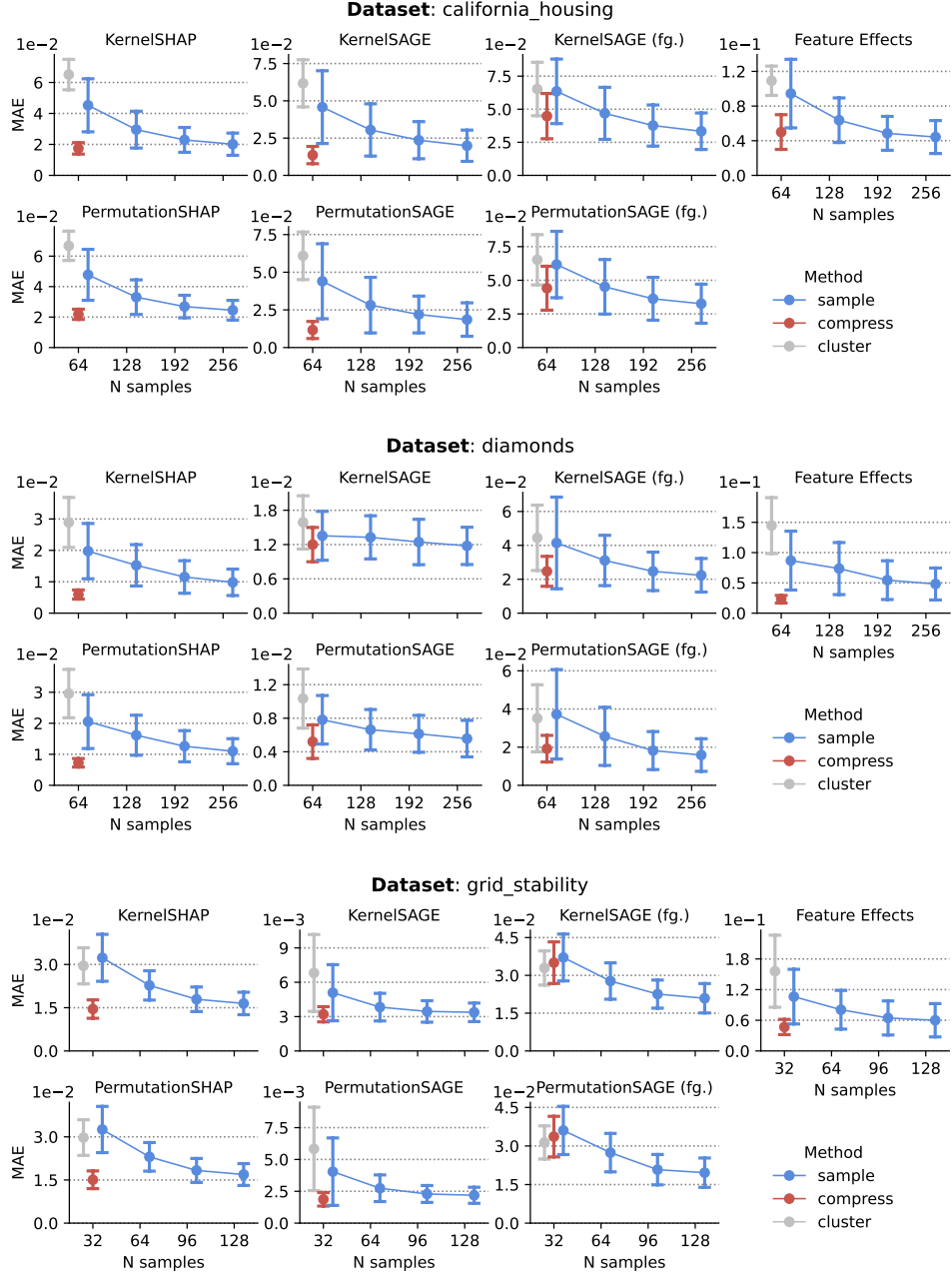


Figure 15: Extended Figure 6 (1/10). CTE improves the explanation approximation error of various local and global removal-based explanations. SAGE is evaluated in two variants that consider either compressing only the background data (default), or using the compressed samples as both background and foreground data (as indicated with “fg.”). (mean \pm sd.)

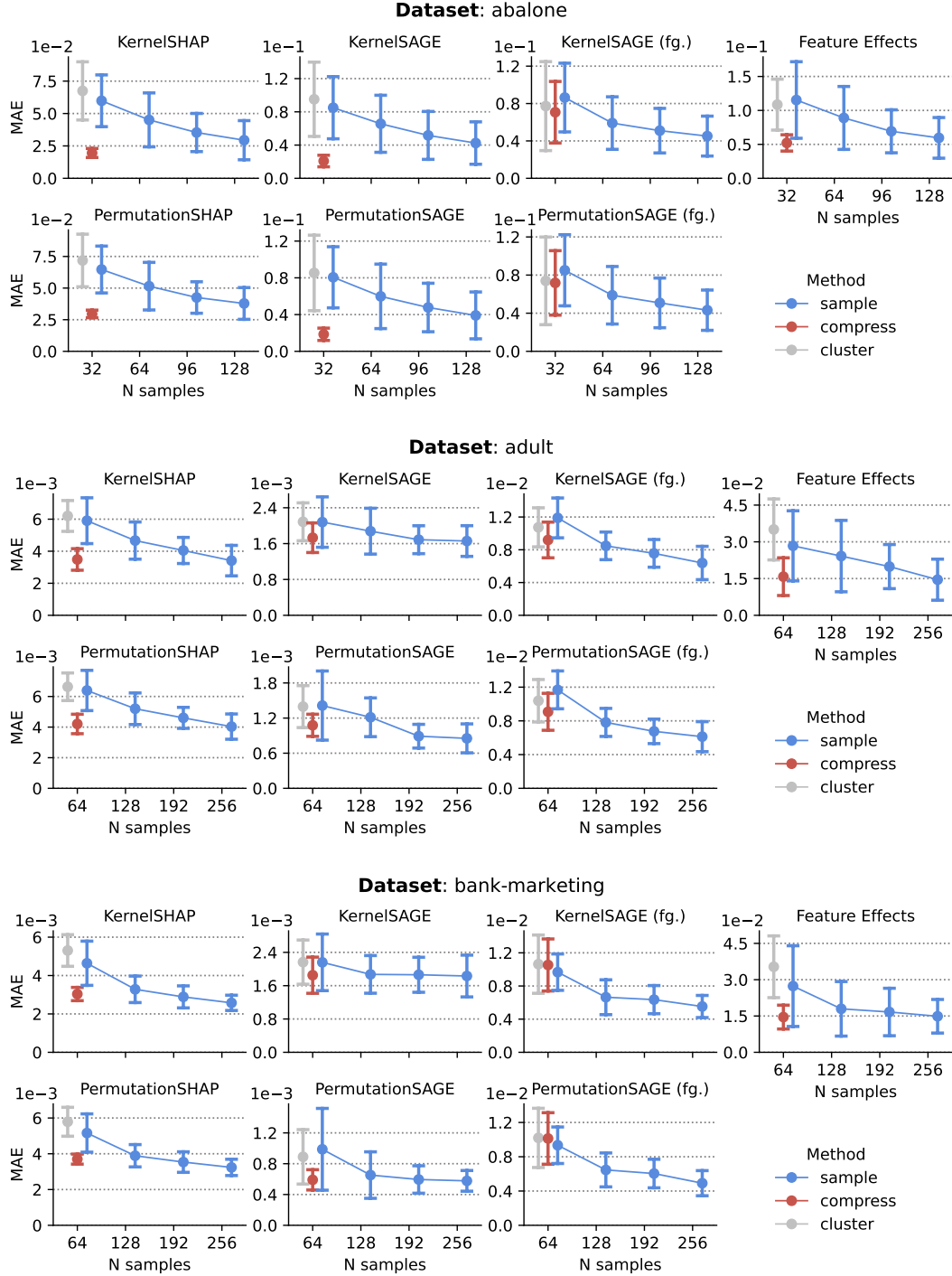


Figure 16: Extended Figure 6 (2/10). CTE improves the explanation approximation error of various local and global removal-based explanations. SAGE is evaluated in two variants that consider either compressing only the background data (default), or using the compressed samples as both background and foreground data (as indicated with “fg.”). (mean \pm sd.)

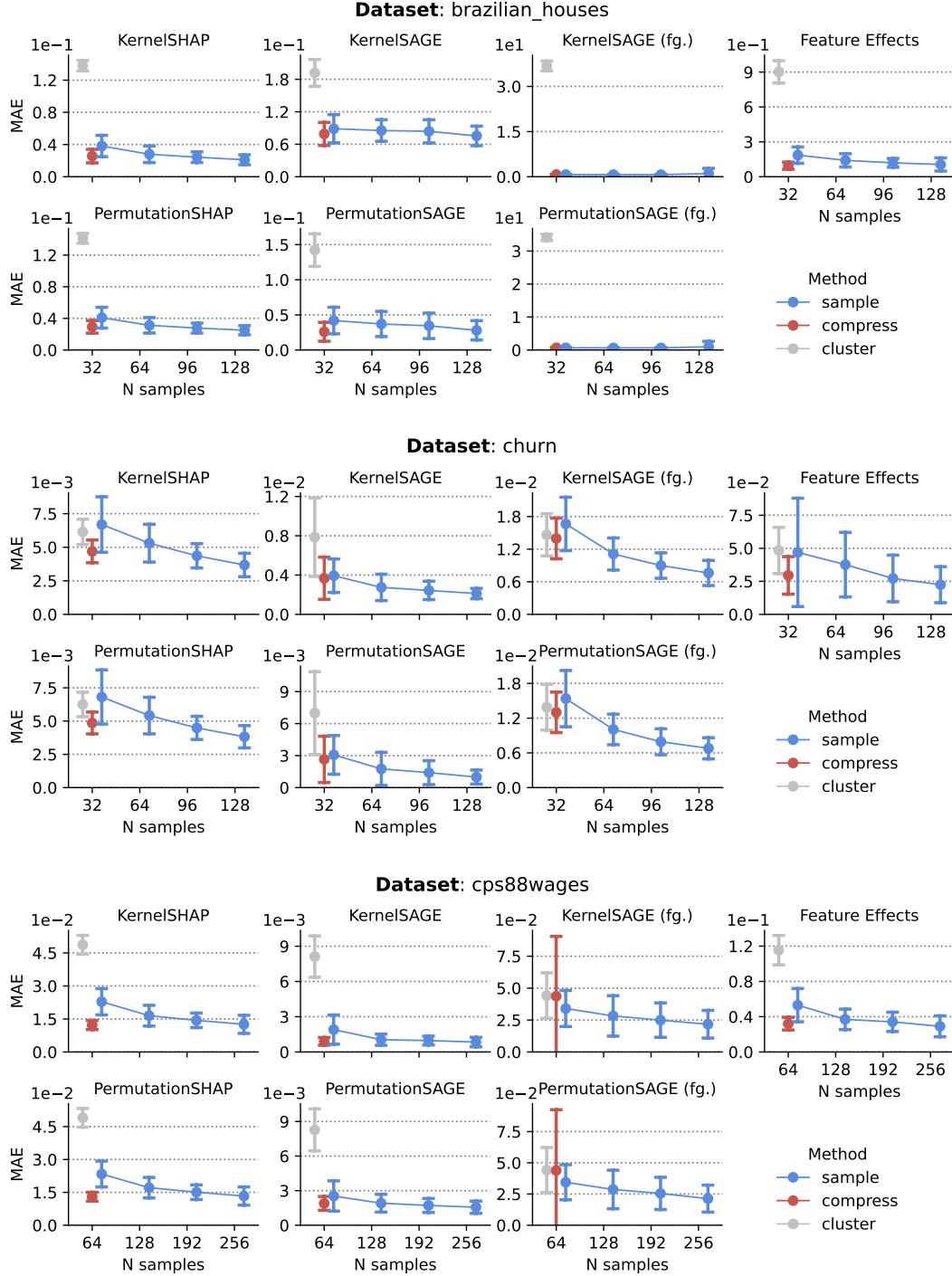


Figure 17: Extended Figure 6 (3/10). CTE improves the explanation approximation error of various local and global removal-based explanations. SAGE is evaluated in two variants that consider either compressing only the background data (default), or using the compressed samples as both background and foreground data (as indicated with “fg.”). (mean \pm sd.)

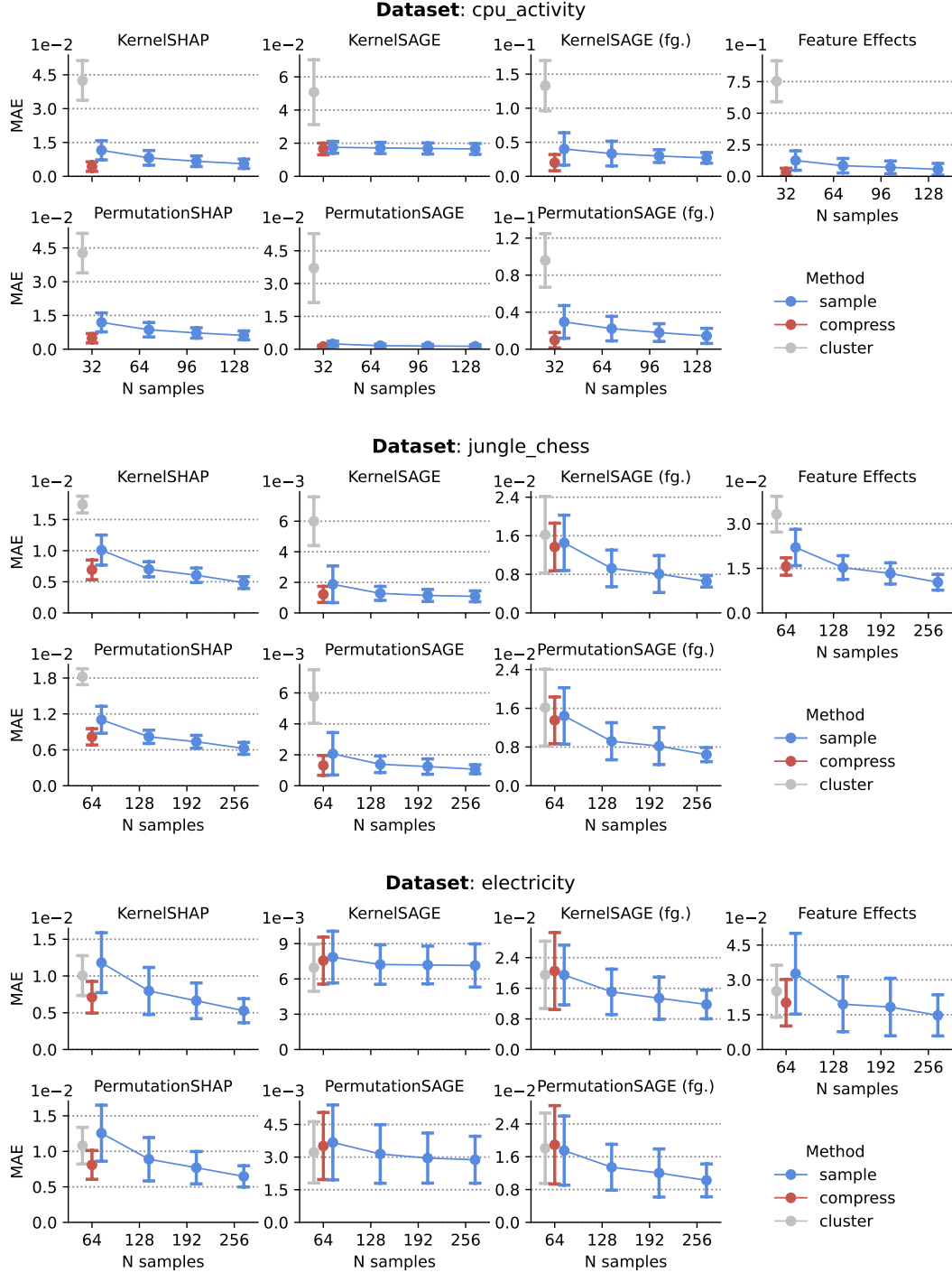


Figure 18: Extended Figure 6 (4/10). CTE improves the explanation approximation error of various local and global removal-based explanations. SAGE is evaluated in two variants that consider either compressing only the background data (default), or using the compressed samples as both background and foreground data (as indicated with “fg.”). (mean \pm sd.)

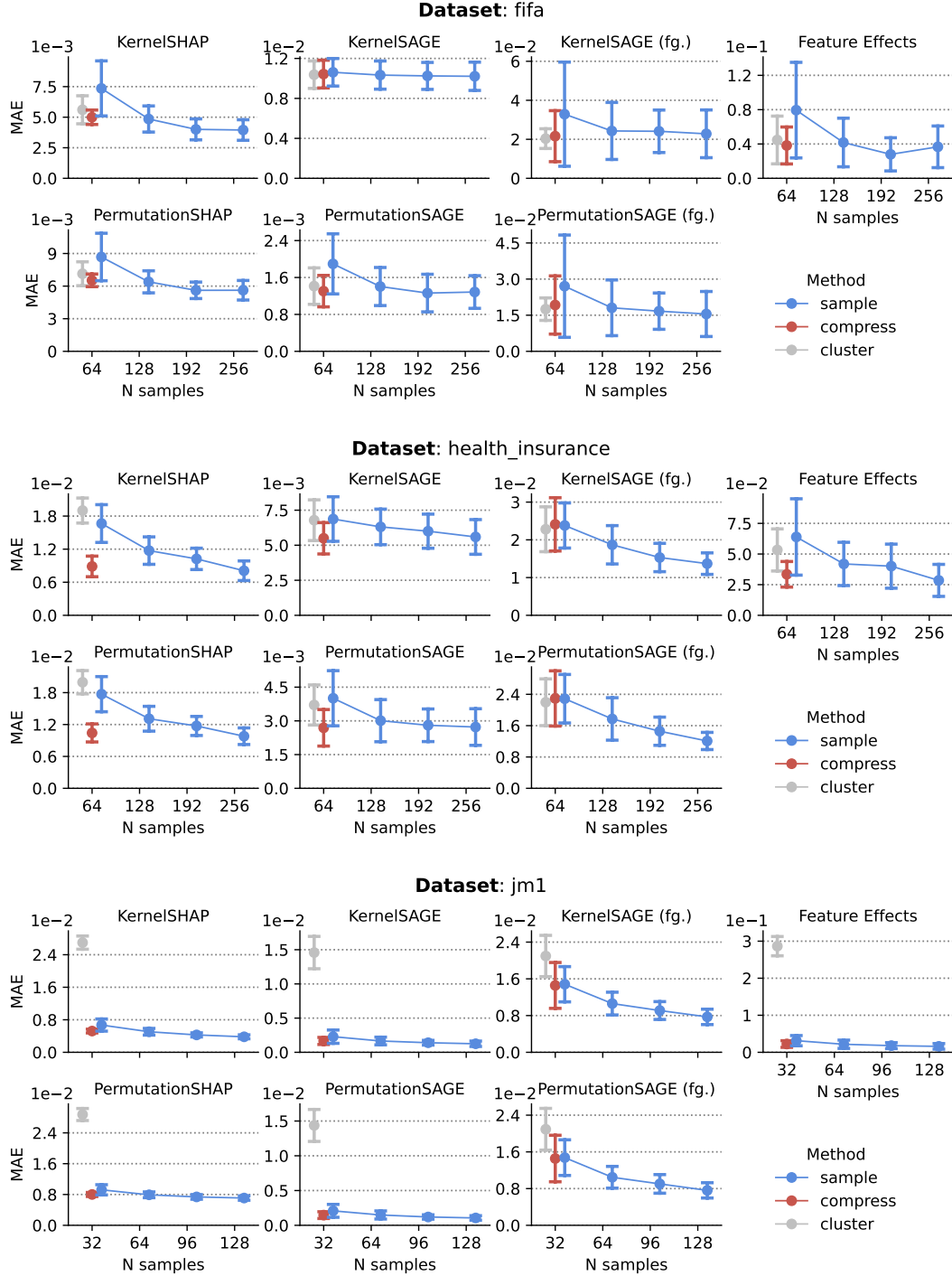


Figure 19: Extended Figure 6 (5/10). CTE improves the explanation approximation error of various local and global removal-based explanations. SAGE is evaluated in two variants that consider either compressing only the background data (default), or using the compressed samples as both background and foreground data (as indicated with “fg.”). (mean \pm sd.)

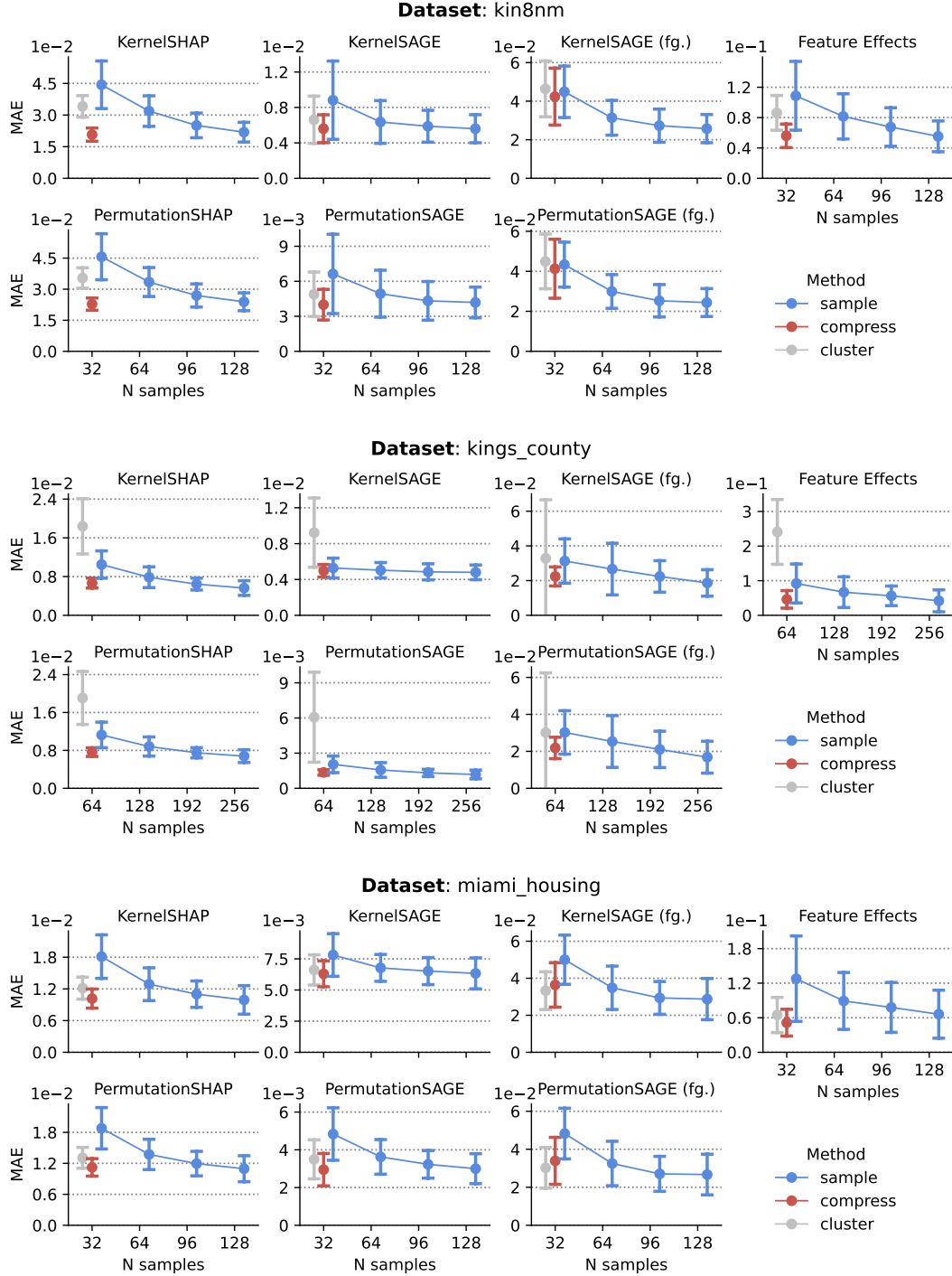


Figure 20: Extended Figure 6 (6/10). CTE improves the explanation approximation error of various local and global removal-based explanations. SAGE is evaluated in two variants that consider either compressing only the background data (default), or using the compressed samples as both background and foreground data (as indicated with “fg.”). (mean \pm sd.)

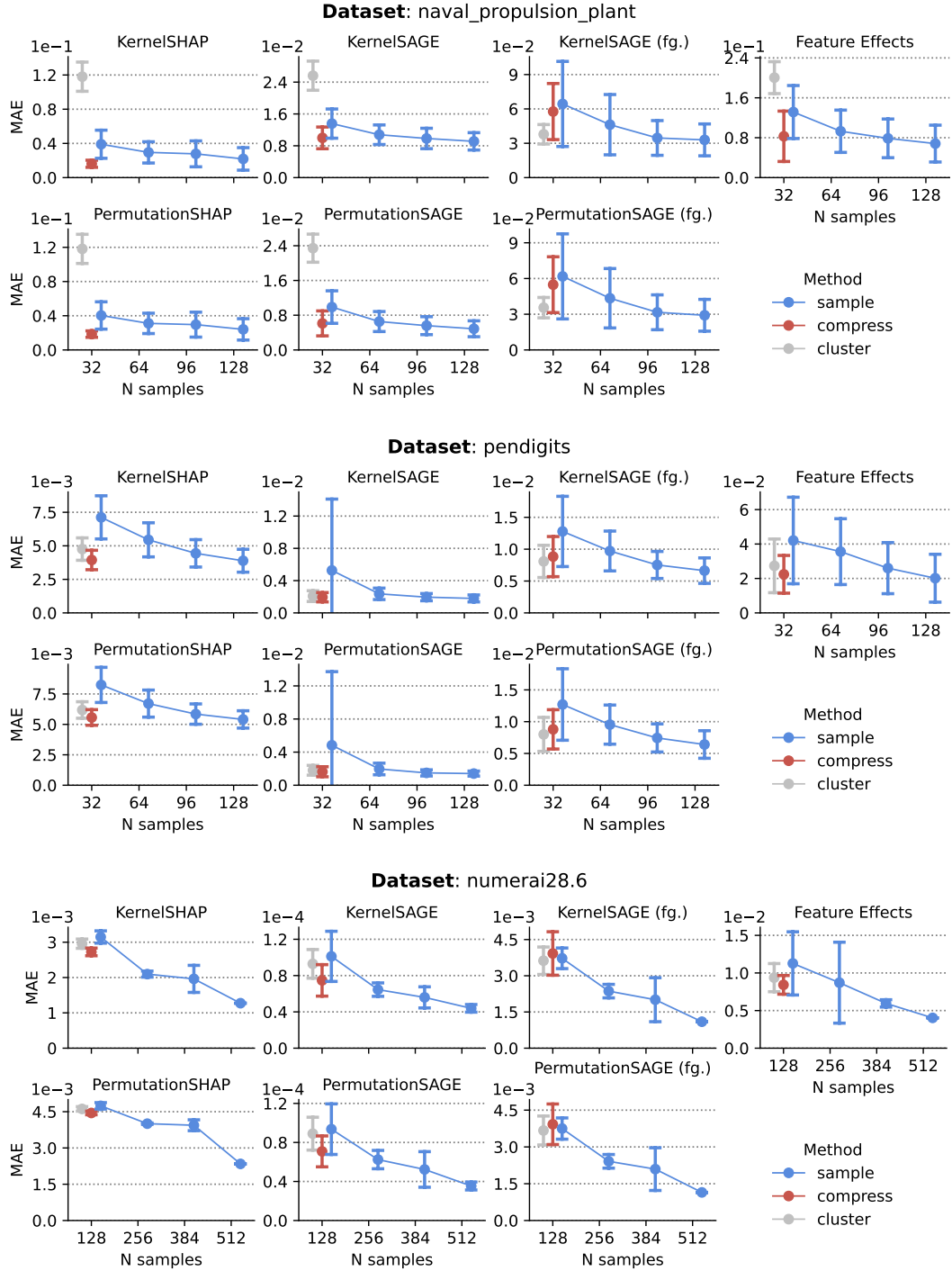


Figure 21: Extended Figure 6 (7/10). CTE improves the explanation approximation error of various local and global removal-based explanations. SAGE is evaluated in two variants that consider either compressing only the background data (default), or using the compressed samples as both background and foreground data (as indicated with “fg.”). (mean \pm sd.)

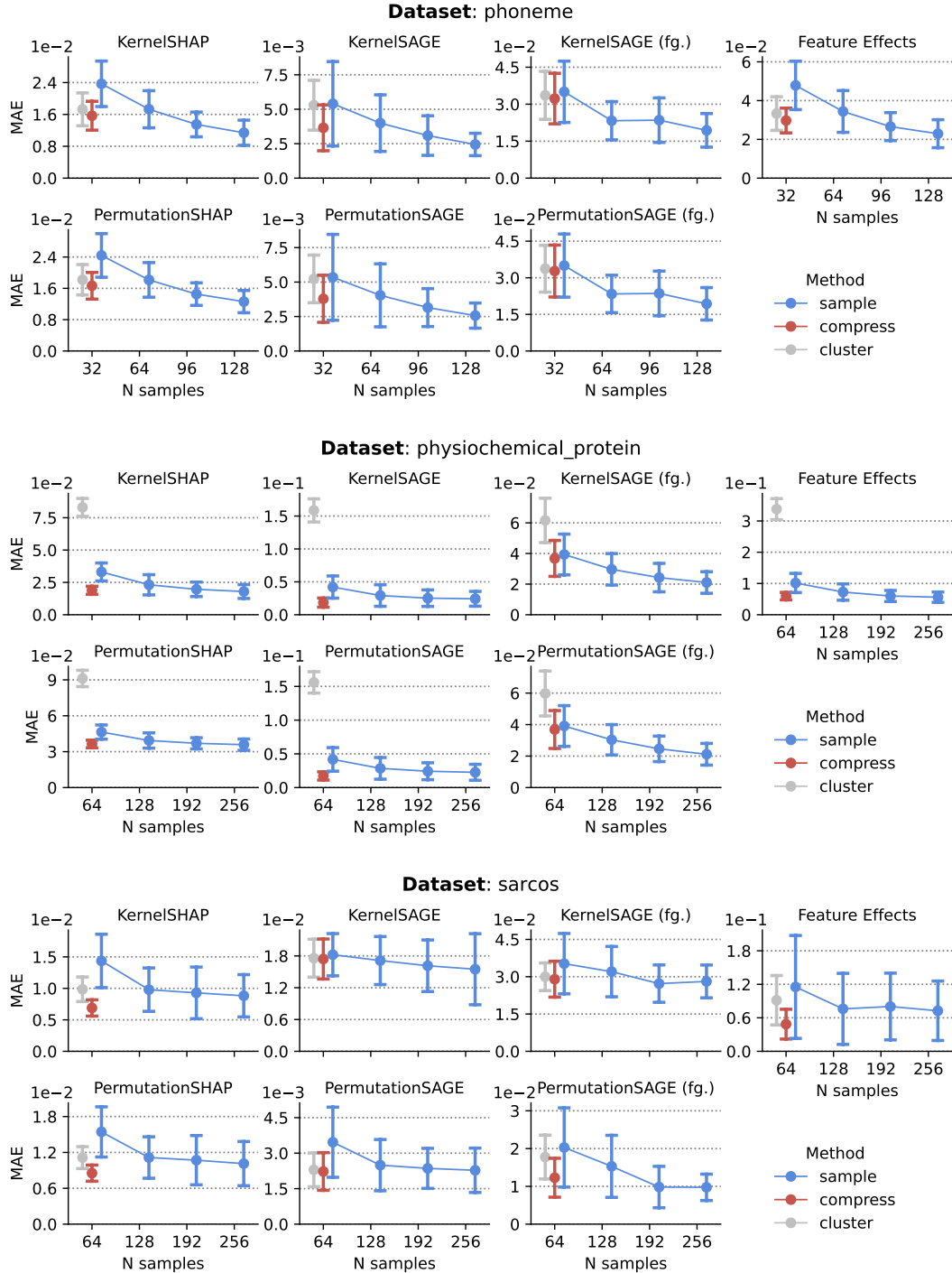


Figure 22: Extended Figure 6 (8/10). CTE improves the explanation approximation error of various local and global removal-based explanations. SAGE is evaluated in two variants that consider either compressing only the background data (default), or using the compressed samples as both background and foreground data (as indicated with “fg.”). (mean \pm sd.)

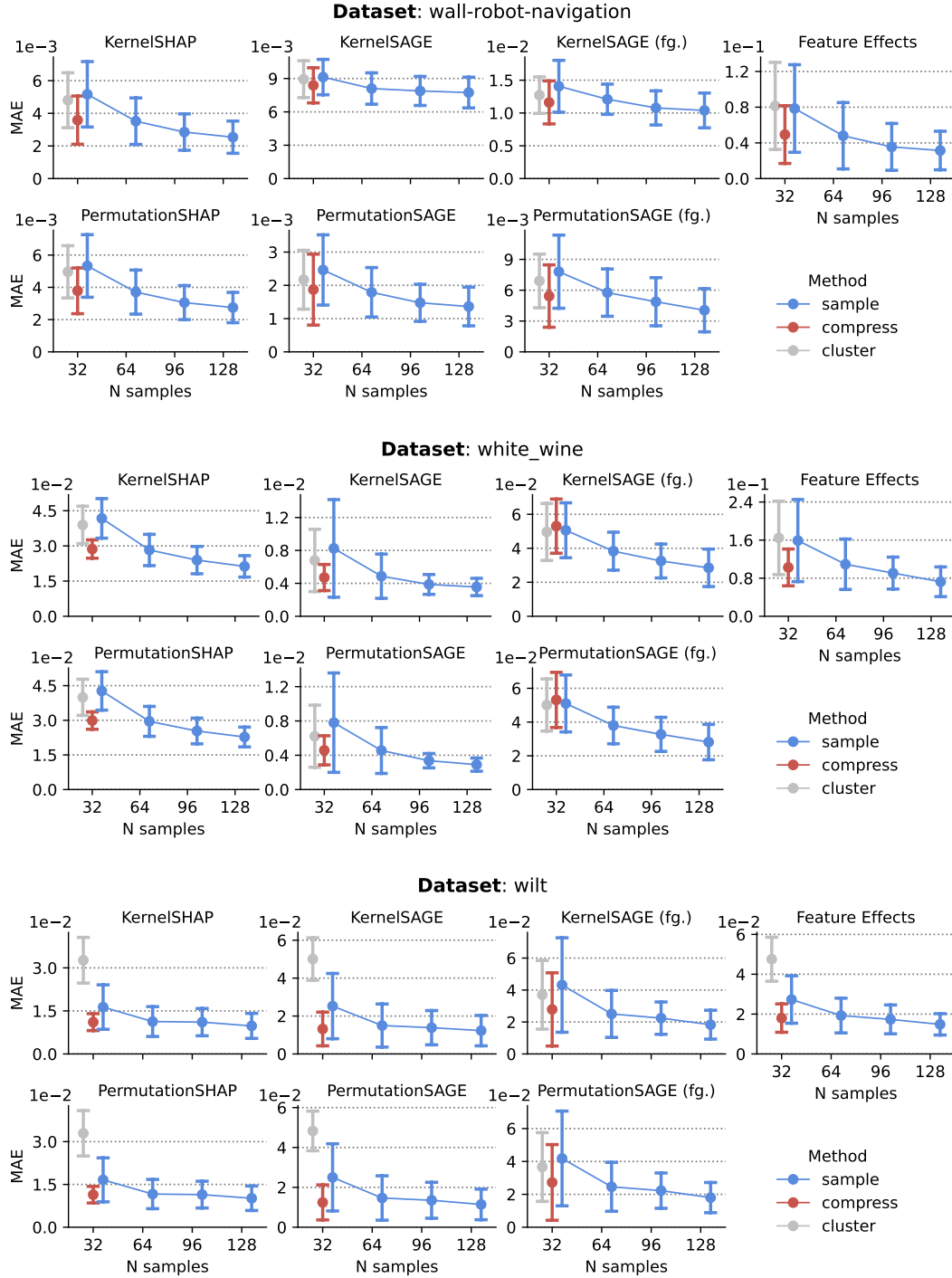


Figure 23: Extended Figure 6 (9/10). CTE improves the explanation approximation error of various local and global removal-based explanations. SAGE is evaluated in two variants that consider either compressing only the background data (default), or using the compressed samples as both background and foreground data (as indicated with “fg.”). (mean \pm sd.)

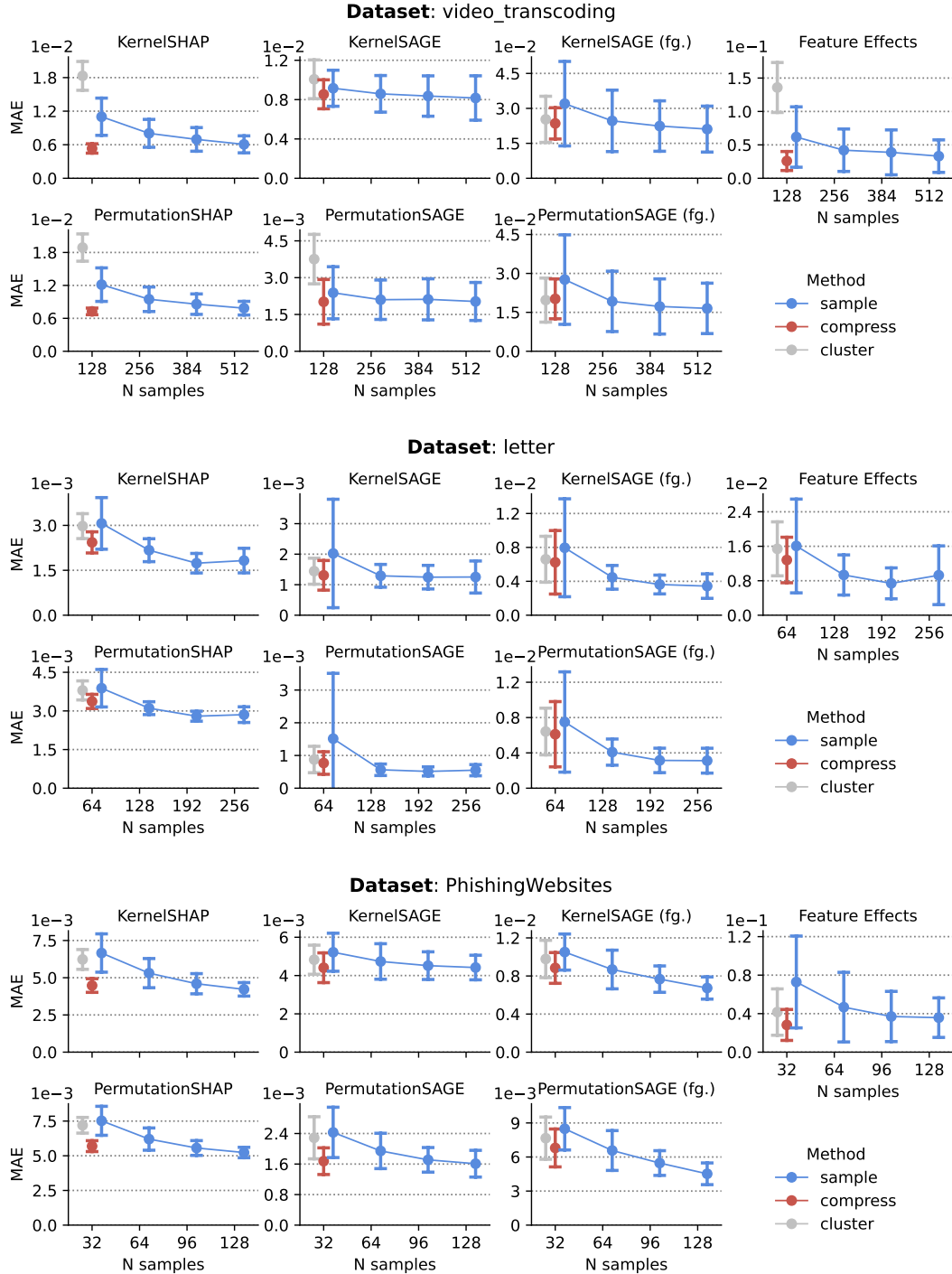


Figure 24: Extended Figure 6 (10/10). CTE improves the explanation approximation error of various local and global removal-based explanations. SAGE is evaluated in two variants that consider either compressing only the background data (default), or using the compressed samples as both background and foreground data (as indicated with “fg.”). (mean \pm sd.)

H COMPUTE RESOURCES

Experiments described in Sections 4.1, 4.2 & 4.5, and Figure 4, were computed on a personal computer with an M3 chip as justified in the beginning of Section 4. Experiments described in Sections 4.3 & 4.4 were computed on a cluster with $4\times$ AMD Rome 7742 CPUs (256 cores) and 4TB of RAM for about 14 days combined.

I VISUAL COMPARISON OF EXPLANATIONS

We provide exemplary visual comparisons between ground truth explanations and those estimated on an i.i.d. and compressed sample in 4 experimental settings.

Figure 25 shows a comparison for KERNEL-SAGE explaining an XGBoost model trained on the `compas` dataset. Figure 26 shows a comparison for PERMUTATION-SHAP explaining a neural network trained on the `compas` dataset, and Figure 27 shows the same on the `heloc` dataset. Note that we show all local explanations at once (not to hand-pick a single one), which might falsely look like a good approximation “on average” when in fact the attribution values in specific cases differ significantly. Figure 28 shows a comparison for FEATURE-EFFECTS explaining an XGBoost model trained on the `grid_stability` dataset, and Figure 29 shows the same on the `miami_housing` dataset. Figures 30 & 31 show exemplary visual comparisons for EXPECTED-GRADIENTS explaining a convolutional neural network trained on the `CIFAR_10` dataset.

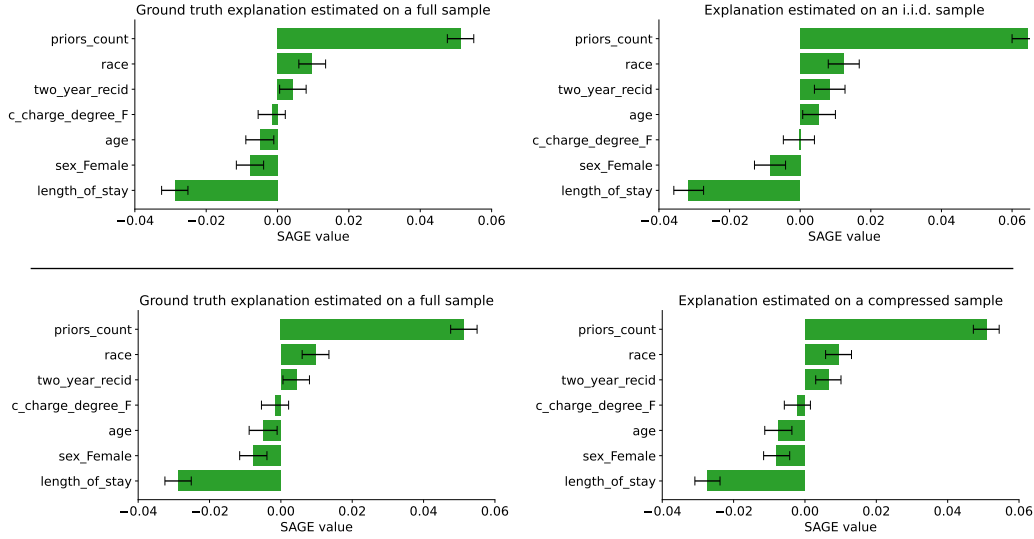


Figure 25: Comparison between KERNEL-SAGE estimated on the full (left), sampled (right top), and compressed (right bottom) subsets of the `compas` dataset. MAE introduced by i.i.d. sampling equals 0.0050 for the importance values and 0.00033 for their standard deviations (error bars), by CTE is 0.0011 and 0.00007 respectively, and so the relative improvement of CTE is 78% in both cases.

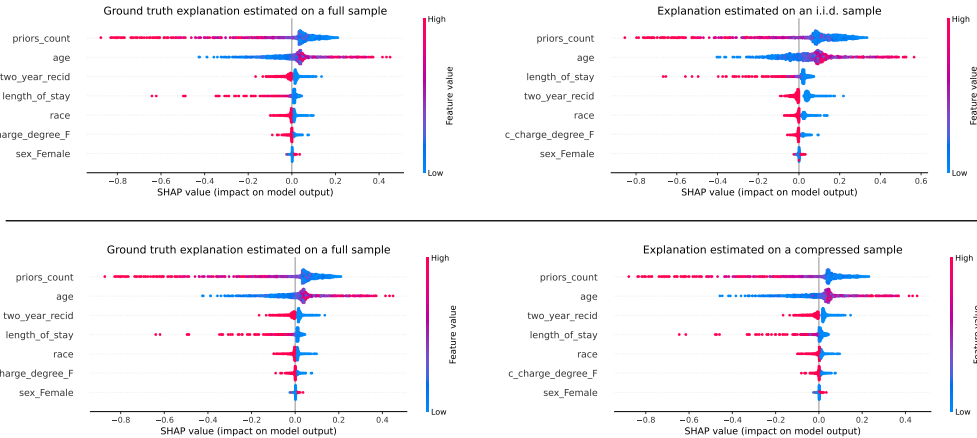


Figure 26: Comparison between all local PERMUTATION-SHAP explanations estimated on full (left), sampled (right top), and compressed (right bottom) subsets of the `compas` dataset. MAE introduced by i.i.d. sampling equals 0.0227, by CTE is 0.0032, and so the relative improvement of CTE is 86%.

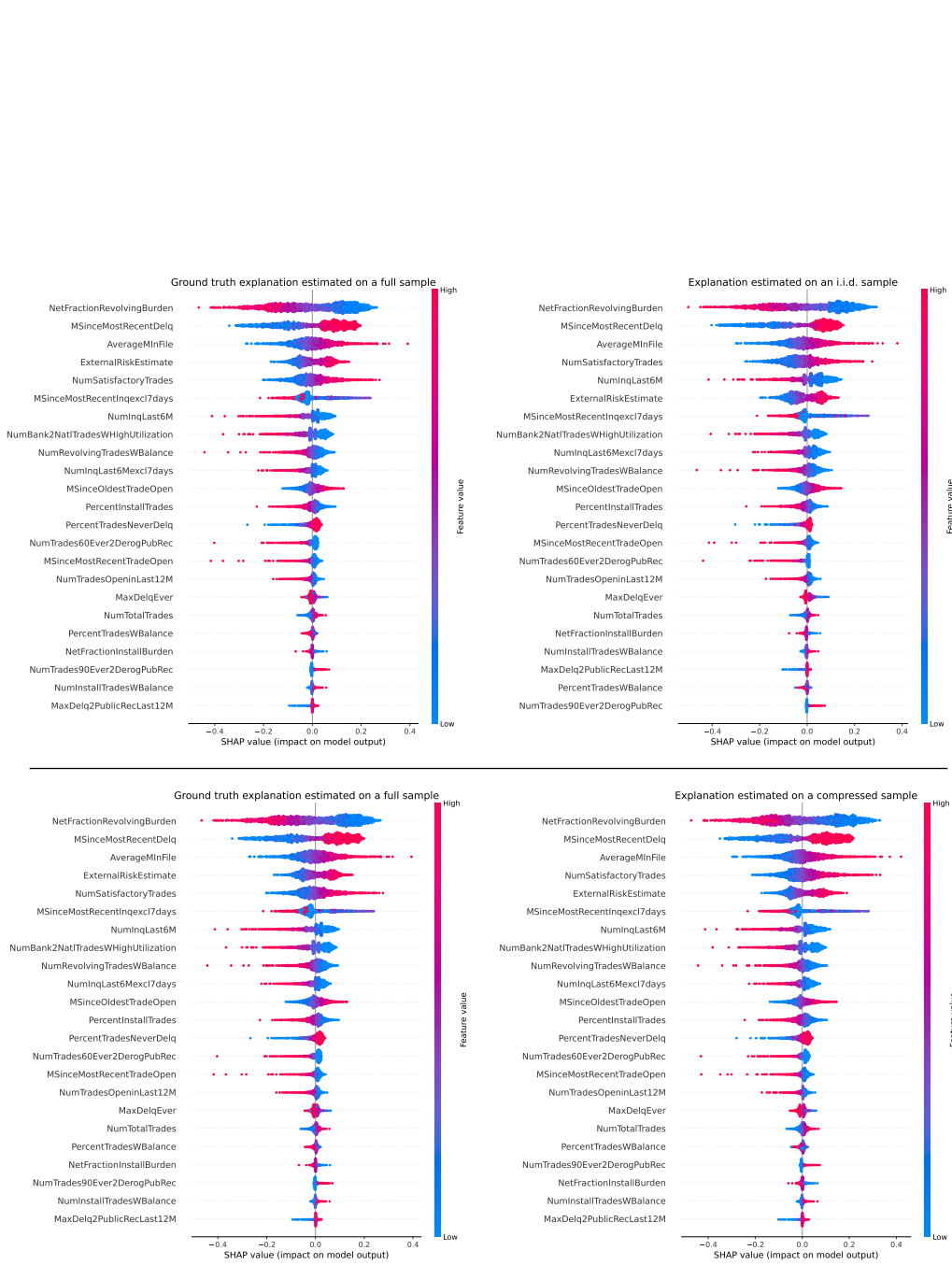


Figure 27: Comparison between all local PERMUTATION-SHAP explanations estimated on full (left), sampled (right top), and compressed (right bottom) subsets of the `heloc` dataset. MAE introduced by i.i.d. sampling equals 0.0087, by CTE is 0.0053, and so the relative improvement of CTE is 38%.

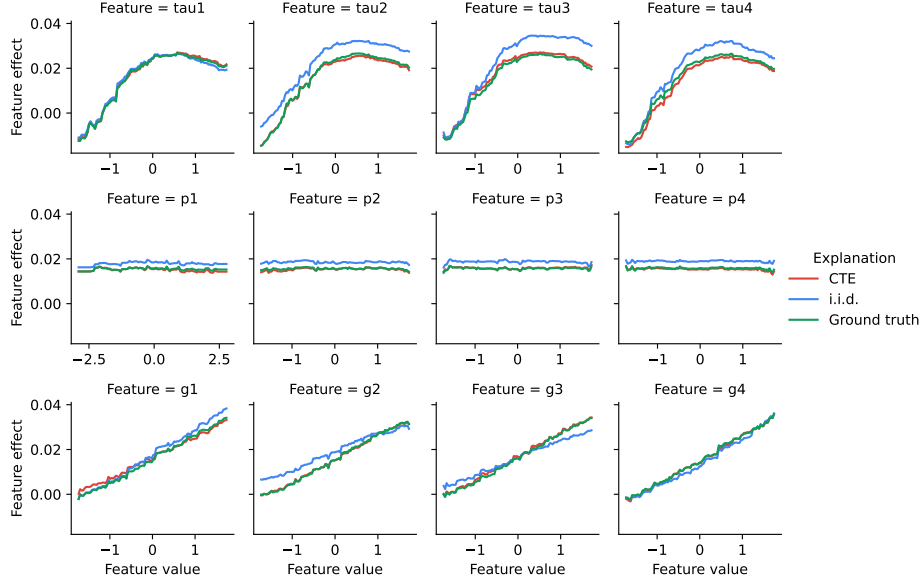


Figure 28: Comparison between FEATURE-EFFECTS explanation estimated on the full (Ground truth), sampled (i.i.d.), and compressed (CTE) subsets of the `grid_stability` dataset. MAE introduced by i.i.d. sampling equals 0.0032, by CTE is 0.0007, and so the relative improvement of CTE is 79%.

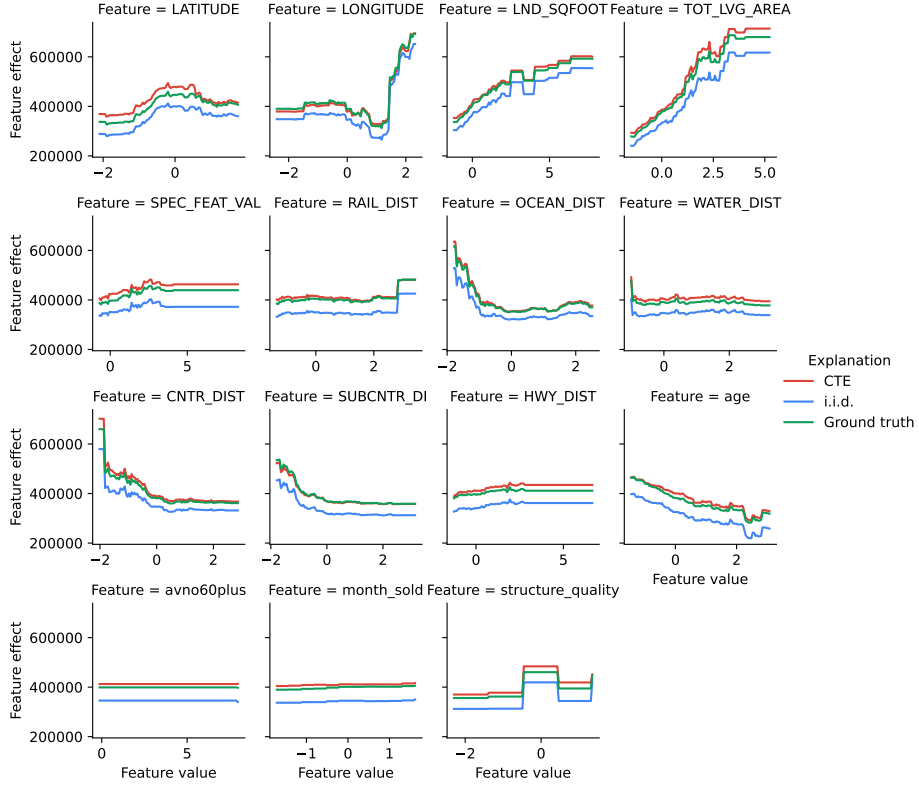


Figure 29: Comparison between FEATURE-EFFECTS explanation estimated on the full (Ground truth), sampled (i.i.d.), and compressed (CTE) subsets of the `miami_housing` dataset. MAE introduced by i.i.d. sampling equals 49766, by CTE is 14031, and so the relative improvement of CTE is 71%.

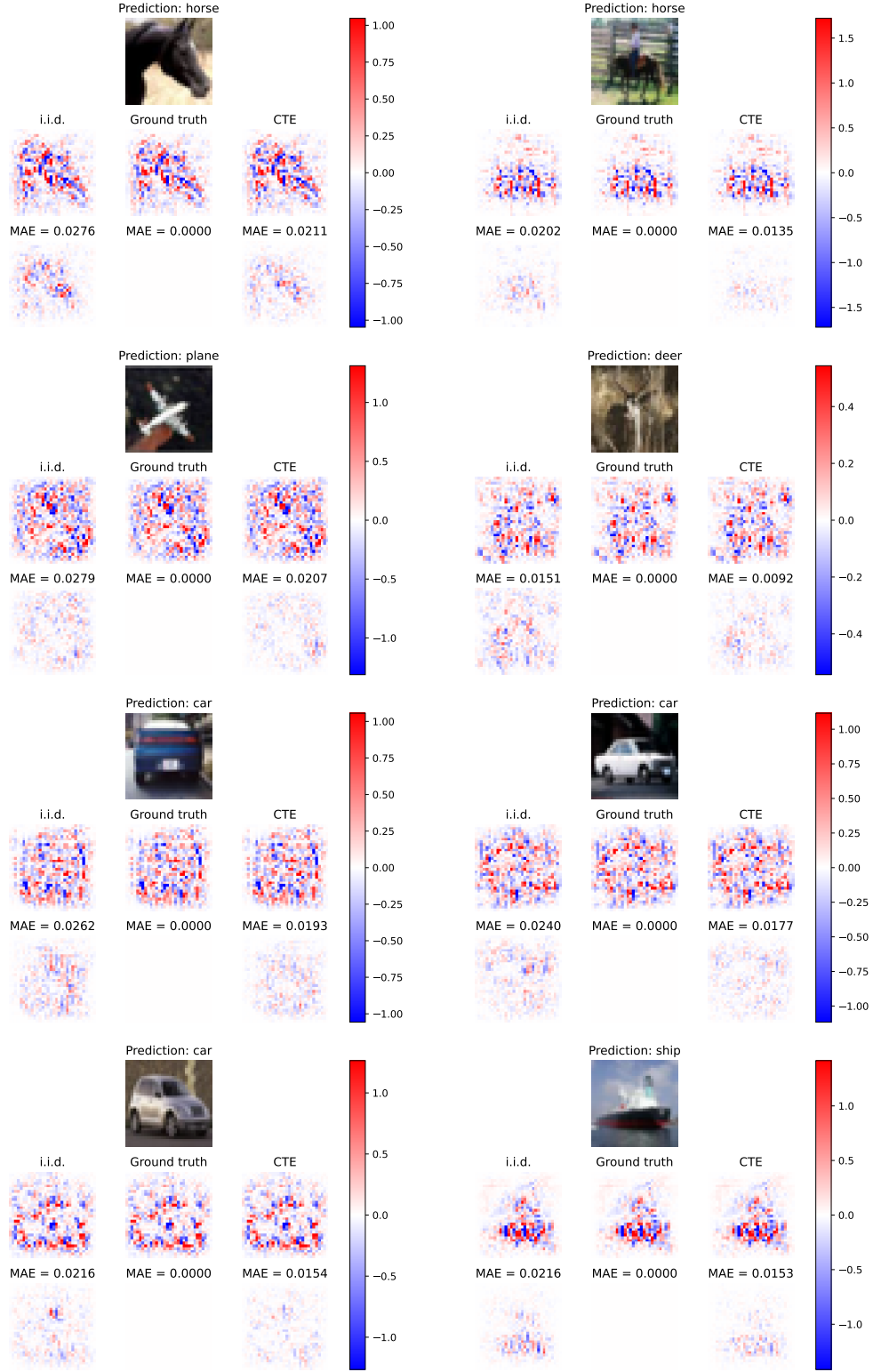


Figure 30: Comparison between EXPECTED-GRADIENTS explanations estimated on the full (Ground truth), sampled (i.i.d.), and compressed (CTE) subsets of the CIFAR_10 dataset. The bottom rows visualize the differences (MAE \downarrow) from the ground truth explanation. All predictions are correct.

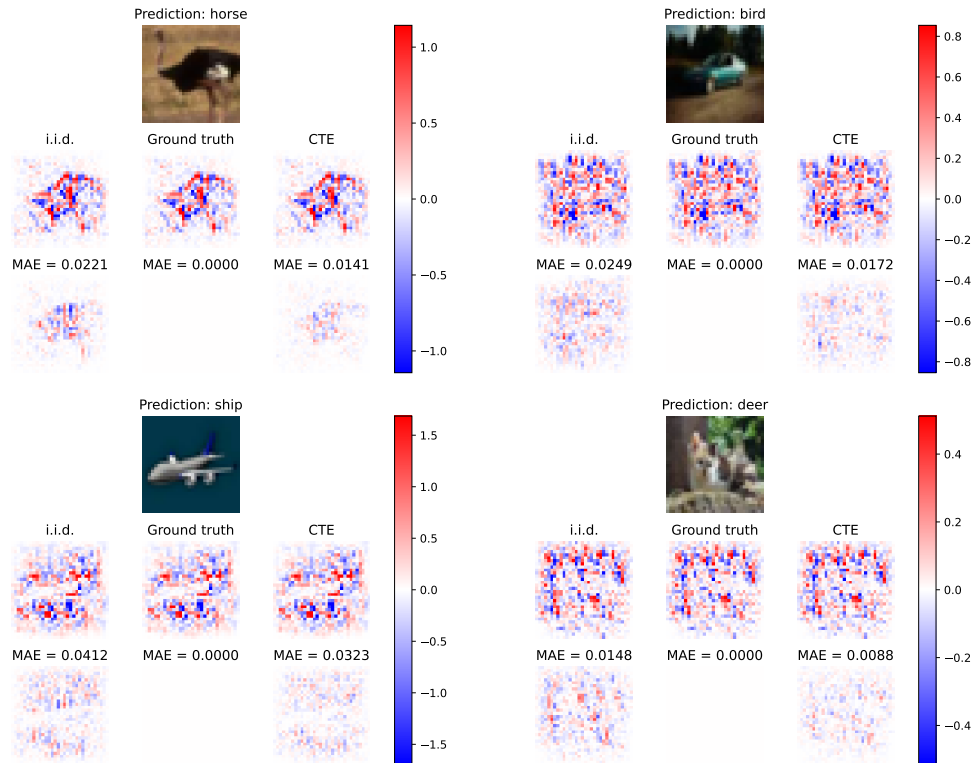


Figure 31: Comparison between EXPECTED-GRADIENTS explanations estimated on the full (Ground truth), sampled (i.i.d.), and compressed (CTE) subsets of the CIFAR-10 dataset. The bottom rows visualize the differences (MAE \downarrow) from the ground truth explanation. All predictions are wrong.